

Response to Reviewer 1

This manuscript presents a model-based climatology of diurnal ozone variations in the stratosphere (50-0.5 hPa) based on the NASA GEOS-GMI chemistry model. This climatology is of significant utility for observational data inter-comparisons and merging activities as it allows to correct for diurnal sampling biases in ozone records. This is a topic of high relevance for readers of AMT. The paper is well written and covers all the relevant details and citations. I recommend publication after addressing my comments below, most of them being minor.

We thank the reviewer for their comments and address each point individually below, as indicated by the bold text. We note that during the review process a model error was identified and a new simulation was run. We reanalyzed the new output, but found for ozone the differences were very small, and did not warrant producing a new climatology at this time. We will periodically update the climatology and include all model updates at that time.

Overall I'm missing a more quantitative discussion on uncertainties and limitations when using the diurnal climatology in different applications. I see three potential sources of uncertainty: (i) model errors, (ii) unresolved inter-annual variability, and (iii) climatology discretization. While (i) is very difficult to quantify, (ii) and (iii) could be assessed in a straight forward manner. The influence of inter annual variability is already discussed in a qualitative way (e.g. Fig S10, differences between 2017 and 2018 outputs) but could be extended to include quantitative estimates. Regarding (iii), a major source of uncertainty could be the relative broad temporal resolution of the climatology (monthly) which may introduce systematic deviations close to the terminator, particularly in the polar regions and at upper stratospheric levels (and above) where photochemistry is relatively fast (intra-month terminator variations are not resolved by the monthly climatology). These errors could be evaluated by e.g. applying the climatology-based diurnal correction to the 0.5-hourly resolved model output itself.

We agree, and we have added a section in the summary (P16 L23-P17 L18) with a more thorough discussion of the potential model climatology errors. We have also made a good faith effort to include reasonable error bars for the climatology. In doing so we analyzed the variability of the high-resolution data going into the climatology (equivalent to re-sampling the model output from the climatology). The standard deviations are large, over 10% in high latitude winter. The climatology will smooth out sub-scale variability related to the diurnal cycle, but we weren't able to isolate that variability from the overall noise. We found very little difference in the standard deviations from hour to hour, suggesting that the longitudinal variability is dominating the variability due to day to day variations in the terminator time (which would cause larger variability in the hour bins near the terminator). We added a cautionary note in the summary with regard to using GDOC near the terminator as well as raised this point in the discussion of the SAGE comparisons.

We have added a figure (now Figure S11) showing the direct differences between the model simulation in 2017 and 2018 as a function of season and latitude at 4 pressure levels. The difference plotted is the max-min difference in local solar time.

Further, an upper vertical limit for a "safe use" of the climatology, would be helpful, particularly when considering that the climatology is provided up to ~80 km (0.01 hPa).

We suggest a safe use range of 30 hPa to 0.3 hPa. This has been added to the text in the same conclusions section, and the actual data set will be truncated.

We have added:

We recommend using GDOC primarily for monthly zonal mean analyses in the pressure range from 30 to 0.3 hPa. Comparisons against the various satellite measurements presented in this study suggest that the climatology captures diurnal variations to well within 5% in most cases. For applications that require accurate knowledge of high temporal and spatial resolution changes in ozone we advise using the original model output (see *Data Availability*).

Specific comments

:p1 l21: "polar summer boundary" -> consider to rephrase to "polar day terminator"

done

p4 l14-15: The reason for the vertical interpolation is not clear. Why switching to a different vertical grid if the climatology is provided on pressure levels and the interpolated levels have a similar vertical resolution as the original pressure levels? Further, Z^* and p_r are not defined.

We have clarified this section, p_r was meant to be Z^* pressure levels. This was done for convenience; we often use Z^* coordinates as a common vertical coordinate when comparing data sets. We noted this in the text (slightly changed from original response):

" Z^* pressure levels are often used as a common vertical coordinate when comparing constituent profiles reported (or modeled) on different pressure/altitude surfaces, and is the vertical coordinate used for other climatologies produced by our group (e.g., the McPeters and Labow [2012] and Labow et al. [2015] profile ozone climatologies)."

p4 l17-20: I guess that local solar time (LST) is meant with "time of day". Can you provide some more details on how the local time binning has been performed? Was the model output at different longitudes (but fixed UT) resampled to local time or was the local time (at fixed longitude) sampled from the output at different UT (and finally zonally averaged)? This question is relevant since the former option (while in principle allowing for better local time resolution) may introduce aliasing effects by e.g. stationary planetary waves while the latter option is much less sensitive to such aliasing effects.

Yes, we mean local solar time, and that has been added to the text. The binning is done by sampling local time at a fixed longitude from output at different UTC. We have added the following details to the text to better explain how the local time binning is accomplished (slightly re-worded from original reply):

"We first average the model output in latitude to reduce the sampling from 1° to 5° . Then at each fixed longitude, latitude, pressure and day, we interpolate in time (at 30-minute resolution) to convert from UTC to local solar time for that longitude. Note that we sample model output from three

consecutive days (in UTC) to get a full local solar time diurnal cycle at each longitude. We then average the diurnal cycles at each longitude to get a daily zonal mean diurnal cycle, and then we average over available days for each month. Finally, for each latitude, level and month, the half-hourly climatological values are normalized to the value at midnight (11:45-00:15 local time bin) and the final climatology is expressed in terms of variation from midnight. We note that GDOC can be re-normalized to any reference time as is most appropriate for a given analysis.”

p4 l25-29: Can you quantify the agreement of the climatologies in Figure S10? The difference of the climatologies for different years could provide a good estimate of the uncertainty range caused by intra-annual variability.

Yes, we have added Figure S11 to the Supplemental, and reference it in the text [see above].

p9ff (Day Night Differences): Apart of Aura/MLS there are also other ozone-observing instruments on sun-synchronous platforms, some of them having different equator crossing LSTs compared to MLS. MIPAS on ENVISAT, for example, took sun-synchronous measurements at 10 am - 10 pm equator crossing LST, in principle allowing to extend the validation of the diurnal climatology by means of observed day-night differences to different LSTs.

This is an excellent idea, unfortunately we did not have time to acquire and familiarize ourselves with the MIPAS data. However we will continue to work to evaluate the diurnal model using additional data sources, and hope to collaborate on efforts with other instrument teams.

p11 l1-4: A possible reason for the divergence between GDOC and SAGE-III above 2hPa could also be related to the limitations of the monthly-resolved diurnal climatology: sunset (SS) and sunrise (SR) times are spread over a certain LST range in the monthly climatology, resulting in an artificial smearing of the diurnal gradient at SS and SR and hence in reduced SR/SS ratios.

Yes, we now note this in the text: “At these levels, the SAGE III/ISS retrieval does not account for the sharp diurnal gradient in the ozone along the line of sight of the instrument. However, GDOC representations near the terminator may also be biased due to smearing of the diurnal ozone gradient in the monthly average as the terminator time shifts within the month.”

p15 l4: the webpage is not accessible.

The corrected web location has been added to the text.

Response to Reviewer 2

Review of: Model-based Climatology of Diurnal Variability in Stratospheric Ozone as a Data Analysis Tool

Stacey M. Frith¹, Pawan K. Bhartia², Luke D. Oman², Natalya A. Kramarova², Richard D. McPeters², Gordon J. Labow

The study is very detailed, and the results are convincing and new. For the first time, the authors demonstrate a feasible way how the effects of the diurnal ozone cycle in satellite and ground observations can be considered and partly removed. Thus, the article is of high interest for the readers of AMT. Future application of a related analysis to other diurnal cycles in other atmospheric parameters might be possible.

We thank the reviewer for their comments and address each point individually below, as indicated by the bold text. We note that during the review process a model error was identified and a new simulation was run. We reanalyzed the new output, but found for ozone the differences were very small, and did not warrant producing a new climatology at this time. We will periodically update the climatology and include all model updates at that time.

I only found minor corrections which are listed below, and I have one question: I would be interested in the dependence of the diurnal cycle on longitude. Did you investigate if topography, convection or land-sea contrast have an influence on the diurnal cycle in the simulation data? Maybe you can add 1-2 sentences about this topic to your article.

Based on comments of another reviewer, we made a good faith effort to establish reasonable error estimates for GDOC, and in doing so did some analysis of the variability going into the averages, including variability in longitude. We found that the variability is quite large and complicated, and unpacking the sources of the variations will take some time. We cannot comment on this yet, but work is ongoing analyzing the model run. We note in the new version that the uncertainty is largest in the high latitude winter, when the variability is greatest, which we associate with higher dynamical variability.

p.1, line 15 what is the meaning of GEOS-GMI?

The acronym has been expanded (and explained) in the abstract

p.2, line 4 Rowland instead of Roland

corrected, thank you

p.2, line 27 plural? Satellite data provide....

corrected

p.4, line 15 0.01 hPa instead of .01 hPa

corrected

p.4, line 20 please inform how the midnight value is defined, e.g., 23:00-1:00

The time resolution of GDOC (and the model output used to construct GDOC) is 30 minutes, thus the midnight time bin is 23:45-00:15. We have added this to the text.

p.8, line10 why did you change to the daily mean as reference?

In general, the reference point can be defined as any time in the cycle (or the daily mean), as is appropriate for the analysis. In this case the measurements are noisy, so normalizing to the daily mean demonstrates the similar structure in each data source but does not rely on the agreement at any single time. This was not made clear in the text and has been expanded upon.

In section 2.1 we added: “We note that GDOC can be re-normalized to any reference time as is most appropriate for a given analysis.”

In Section 3.2 we added (revised wording from original response): “The satellite data tend to be noisy, so we normalize to the daily mean rather than to values at a specific time.”

p.8, line 19...measured by the satellite instruments.

corrected

p.11, line 3 line of sight?

Yes, corrected

p. 14, line 2...because no observational data source...?

corrected

p. 14, line 14 The sentence is not so clear. Perhaps "transits" instead of "transition"?

Thank you, we changed the wording to “shifts”

Response to Reviewer 3:

This manuscript describes the (GEOS-GMI) global model climatology (12 monthly sets) regarding ozone diurnal change as a function of local time for various latitude bins and pressure values. The chosen time step (resolution) is a half-hour. Model values are compared to various data sets, mostly from satellite-based ozone measurements with different spatio-temporal samplings. Most of the comparisons seem to validate the model results, even if there are a few discrepancies that are not completely explained. This model climatology is publicly accessible (or will be), and this offers a useful tool for other investigators, to try to improve certain upper stratospheric and mesospheric ozone comparisons.

We thank the reviewer for their comments and address each point individually below, as indicated by the bold text. We note that during the review process a model error was identified and a new simulation was run. We reanalyzed the new output, but found for ozone the differences were very small, and did not warrant producing a new climatology at this time. We will periodically update the climatology and include all model updates at that time.

General Comments

The paper is generally well-written, clear enough, and fairly thorough in the set of comparisons that are provided for validation. It does not purport to solve in detail every intercomparison's discrepancies. However, the lack of error bar discussion does raise some concerns, regarding the applicability for users; while the comparisons do indicate that the model provides a good representation of the true diurnal changes for ozone, the small differences that come up in terms of inter-instrument trend comparisons, for example, might still be "explained away" by uncertainties in model-based corrections, even after diurnal adjustments. Other uncertainties involve actual line-of-sight gradient issues, not just for the model results, but also for satellite-based retrievals, in particular, for solar occultation results (for which some attempts have been made to adjust for such gradients, but not as a general rule). These issues are the more difficult aspects, but this does not preclude, in my view, publication of this sort of manuscript. I ask for minor clarifications and some attempts (at least) at a better discussion regarding uncertainties, see my specific comments below. I also provide editorial-type comments, mostly as suggestions or corrections.

We thank the review for their comments and have added a good faith effort at reasonable error bars, as described further below. We also add some additional summary comments that try to clarify the conditions most applicable to GDOC (slightly revised from original response):

"We recommend using GDOC primarily for monthly zonal mean analyses in the pressure range from 30 to 0.3 hPa. Comparisons against the various satellite measurements presented in this study suggest that the climatology captures diurnal variations to well within 5% in most cases. For applications that require accurate knowledge of high temporal and spatial resolution changes in ozone we advise using the original model output (see *Data Availability*)."

Specific Comments

One somewhat confusing detail has to do with the normalization time. For example, pg. 4, line 20, and pg. 6, line 4 refer to midnight as a normalization time. The Fig. 1 caption agrees with this description.

However, the caption for Fig. 2 refers to 1:30 am as the normalization value, and so does Fig. S9. It would be good to clarify why there are these different normalization times, or if they should be the same. It probably does not matter too much, if different Figures are normalized slightly differently, but I found this confusing, so if something is written in error there, please correct.

**

We have added a sentence (in Section 2.1 and in the Summary) that says GDOC can be normalized to any time (or to the daily mean time) as needed for a specific analysis. That being said, the normalization to 1:30am in the figures was a carry-over from some Aura MLS analysis, and is unnecessarily confusing as the reviewer points out. We have updated the plots to be normalized at midnight for consistency. In Figure 3 for example we deliberately chose to normalize to the daily mean, which, for the satellite data, was less noisy than the values at any particular time, and thus allowed for a better demonstration of the similar overall structures of the cycles, despite the noise.

2) Error bars are not always described (e.g., for Fig. 3), or justified (e.g., why not use standard error in the mean rather than standard deviation for Fig. 5 and Fig. 7, and similar Figures in the Supplement?). When using a very large data set (e.g., 2004-2018 Aura MLS data in Fig. 5), the random source of error will basically disappear. As an aside, geophysical variability probably accounts for some of the year-to-year differences; differences in day/night temperature or H₂O ratios, for example, could have some impact on O₃ abundances and O₃ diurnal change. In the mid- to upper stratosphere, N₂O day/night variability from year-to-year (or month-to-month) could impact ozone and its day/night ratios. Some comments about why the authors chose to use standard deviations rather than errors in the mean would be welcome (is it to try to encompass such geophysical variability, which would be ignored in a standard error minimum type of error representation?). Maybe the standard deviation is indeed a more acceptable way to try to encompass sources of error, but I would welcome a brief comment regarding this point somewhere.

We have added error bars and descriptions to all the relevant plots. In general, standard error of the mean is the statistic shown. In the Aura MLS profile day/night comparisons we wanted to highlight the year to year variability, so the standard variability is shown for the year to year variability only. This is now stated in the text and the figure caption.

For GDOC itself we have added an uncertainty estimated based on the standard error of the mean. With so many measurements going in, the standard error of the mean was unreasonably small. We therefore computed correlations lagged in longitude to get an idea of the number of independent spatial measurements going into each bin, and based the standard error of the mean off that number (360 longitude points was reduced to 12, we also assumed all measurements within a 5 degree latitude band were correlated). The resulting standard error of the mean varies up to 2%. We include a new figure (Figure 3) as well as error bars on the GDOC profiles.

3) In some places, there is a mention of vertical "integration" of MLS data to match the vertical resolution of SBUV. This sort of smoothing is best done via the use of MLS Averaging Kernels (and MLS a priori data), although this can be somewhat tedious. The details are not mentioned here, but probably some indication of the "smoothing" or averaging process should be provided. Is there no smoothing in the Figure 5 results? Maybe errors in this, or omission of this, could lead to differences or discrepancies in the results (?). [It would also make more sense to smooth the MLS data sets for day and night and then calculate the ratios, than to smooth the MLS ratios, not that this is what was done].

We typically use the SBUV averaging kernels applied to MLS, so that the degraded MLS correctly approximates the lower SBUV resolution. In this analysis we did not apply the averaging kernels, but we tested the results and found it does not make a difference. The impact of the averaging kernels is much smaller than that of the diurnal correction. There is no smoothing in Figure 5. The MLS are simply interpolated onto the Z*star pressure grid. The following has been added to the data section: "OMPS NP and SBUV report ozone as partial column densities (in DU) in pressure layers. Number density and mixing ratio profiles are integrated to give cumulative column densities with pressure, which can be interpolated to re-partition the partial columns to match the SBUV/OMPS vertical sampling."

4) For Figure 6 in particular, the model could be used, in theory at least, to calculate line-of-sight differences in ozone signal for a solar occultation measurement, using small time steps for such a "ray-tracing" calculation, including height-dependence. Comparisons to a case assuming homogeneous line-of-sight ozone abundances, which is often assumed in retrievals, could be made. In theory, the sign of the differences in this case (model versus observations) could thus be ascertained. The authors could at least expand on this by stating that these comparisons are difficult because of not only the model calculation aspects but also the satellite retrieval aspects (they do mention the model, it seems, but not the satellite retrievals explicitly). It is alright to state that such detailed analyses are needed to better ascertain whether the model and data really disagree, even if the more detailed work is not pursued in this manuscript. Also, I wonder if one would not need finer sampling of the model in local time to match the fast changes at sunrise or sunset...(I am not asking to necessarily carry this research out in detail here).

Yes, one would likely need a finer resolution diurnal information to untangle the diurnal impact on the occultation retrieval. This is actually the point we were trying to make (about the retrieval) but it was not clear in the original text. We have re-worded as follows: "At these levels, the SAGE III/ISS retrieval does not account for the sharp diurnal gradient in the ozone along the line of sight of the instrument. However, GDOC representations near the terminator may also be biased due to smearing of the diurnal ozone gradient in the monthly average as the terminator time shifts within the month. Also, as noted above, there is some variation between GDOC, WACCM and observations in the SR/SS pattern in the tropics. Nevertheless, these differences suggest potential discrepancies between SAGE III/ISS sunrise and sunset measurements that are currently being explored (R. Damadeo, personal communication, 2019). The purpose of this work is not to evaluate SAGE III/ISS observations but to demonstrate how GDOC can be used in such evaluations."

Also in the last paragraph we note that for studies requiring higher resolution accuracy may need to use the model output directly.

5) Error bars: I would note that there are no error bars in Figure 6, so either they are too small, or just not calculated (as a standard deviation of the ratios, as done in other Figures), probably the latter. Including such error bars would make sense, however. Also, the error bars in Fig. 8 seem to be indicated by dashed lines, a different format, but please explain these ranges in the caption. Also, in Figure 9, maybe a standard error in the mean values as a function of time here would be more appropriate, but no error bars are shown; some comments regarding this (or actual error bars) would be appreciated as well. I expect that the volume of data used for these comparisons (for each specific month) is large enough to ensure that random errors become negligible.

**

We have added error bars to Figure 6. In the case of the SAGE data, the standard error of the mean for the sunrise and sunset averages is computed, then the root mean square of the two errors is used as the final uncertainty (because of sampling it is the ratio of the average not the average of the ratios). In the case of GDOC, the model errors for each sub-sampled SAGE profile are collected and the root mean square of all the sunrise and sunset error profiles are computed first, then the root mean square of the resulting sunrise and sunset error profiles is computed, as was done for SAGE.

In Figure 9 we plotted the standard error of the mean, but it is smaller than the thickness of the line. We added a comment in the caption explaining this.

Editorial-type Comments / Suggestions-

We thank the reviewer for their corrections and suggested changes, which made the manuscript read much better. Unless otherwise noted, we made all changes as suggested.

Page 1

L14, add a comma after "this issue".

L16, change "applied in" to "applied to".

- Page 2

L3, decide if use ODSs or ODS (I would follow the WMO Report type of writing, so probably ODSs for plural, elsewhere also)

L6, change "has been" to "have been".

L24, "to analyze the ozone diurnal cycle at ..."

L28, change "Atmospheric" to "Atmosphere".

- Page 3

L3, "non-sun-synchronous"

L6, change "source" to "sources"

.L7, I suggest "Also, these missions do not provide full global coverage."

L25, "as well as to that from..."

- Page 4

L19, it seems that "semi-hourly" should replace "hourly" here, since you use 30 minute model time steps.

We used the wording "half-hourly"

- Page 5

L7. You mention OMPS NP and OMPS LP. You also later refer to OMPS profile data and mention NP (top of page 12). Please clarify which data set is being used, NP or LP (or both?), as this was not quite clear enough; maybe this mainly requires a change on page 12. If the datasets are used as mentioned (LP for one plot, NP for another), please clarify (briefly) why one should use LP versus NP or vice-versa (what are advantages/disadvantages of NP versus LP?).

We have added some explanatory text. OMPS NP and LP are separate instruments but on the same platform; LP measures high resolution vertical ozone profiles, while NP is a nadir view instrument that measures in broad layers. Both are useful in their own right, so in this work we are demonstrating comparisons with both. The nadir instrument (OMPS NP) is best for total ozone and continues the SBUV nadir ozone record dating back to 1970. The LP provides very high resolution data, but as a new instrument it doesn't have the stable record of OMPS NP and its predecessors.

We have added: "While OMPS LP is a limb scatter instrument that measures at high vertical resolution, OMPS NP is a nadir backscatter measurement with a broad vertical resolution in the stratosphere. Higher resolution instrument measurements (SAGE III/ISS, MLS, OMPS LP) are often used to help evaluate the lower resolution nadir instruments. This is critical to ensure OMPS NP can continue the 40+ year record of trend quality ozone from the SBUV series of nadir instruments."

- Page 6

L8, add commas "...very little, if any, variation..."

L12, add a comma after "Parrish et al. [2014]".

L15/16. However, SMILES data also suggest that ozone is decreasing..."

L22, add a comma after "Figure 4a]".

L28, either say "variations greater than" or "variations of more than"

- Page 7

L2, authors suggest that the

L8, Delete "Supplemental"

L9/10, matches the higher summertime amplitude model diurnal cycle reported by Studer...

L11, panels of Fig. 1 show the diurnal cycle...

L14, change "greater" to "more".

L18, but with larger afternoon values at 3 hPa

L22, delete "Supplemental" [also, it is a bit strange to refer to S1 after you referred to S2 earlier]

- Page 8

L20, relative maxima.

L22, relatively high ozone value.

Replaced sentence with "Finally at 5 hPa the stratospheric pattern dominates, with measurements and climatology showing the highest daily values in the mid-afternoon."

- Page 9

L7, add a comma after "this comparison"

L8, shows the ratios of daytime to nighttime averages

L17, amplitude of those in the MLS data, with ratios generally ...

Replaced sentence with "Overall GDOC closely matches the spatial pattern and amplitude of the ratios measured by MLS, with agreement generally to within 2%."

L18, near 1 hPa, we note a local minimum in ...

L19, local minimum

- Page 10

L2, delete "Supplemental"

L23 and L26, (maybe) change middle latitudes to midlatitudes

middle latitudes changes to mid-latitudes

- Page 11

L3, change "site" to "sight"

L18, add a comma after OMPS NP. also, please state briefly how the conversion for MLS O3 profiles from pressure to altitude is made.

We have added the sentences "Aura MLS profiles are converted from volume mixing ratio on pressure surfaces to number density on altitude surfaces using co-located MERRA-2 temperature and pressure data." to this section.

L20, change "show" to "shows"

L24, influence of the diurnal cycle on such analyses

- Page 12

L11, please add a sentence or two describing the "known bias pattern" for nadir UV instruments... Not everyone is familiar with what this means, and readers should not have to try to dig this out from other references (top-level information at least); "bias pattern" versus what? (in general?).

We have re-worded this section as follows: “The remaining pattern of differences is consistent with biases previously reported in the nadir UV backscatter series of instruments relative to satellite (SAGE II, UARS and Aura MLS) and ground-based (select microwave and lidar) data [i.e. Kramarova et al., 2013; Frith et al., 2017]. Namely, the nadir backscatter instruments tend to have a negative bias below 10 hPa and above 2.5 hPa, and a positive bias near 7 hPa.”

- Page 13

L10, please specify which instrument’s results show a larger (or smaller) amplitude, is it MLS or SBUV, since the differences do not provide the reader with this information. One would think that the finer resolution instrument might provide a larger amplitude, although the broader vertical extent of the SBUV views means that this is actually not obvious.

In this case, MLS is a reference instrument and does not change between the upper and lower plots. The SBUV has been “adjusted” to match the MLS measurement time of 1:30pm. We have added a statement in the text clarifying that only SBUV changes.

L13, delete "Supplemental"

L24, change ozone levels to ozone values

L25, expressed as ratios to the value at midnight

- Page 14

L11, change "depicts" to "exhibits"

L27, suggesting that the representation...

- Page 21, change Froidevaux to Froidevaux et al.; also change Livesay to Livesey.

- Figure 1: the caption says "30 hPa to 0.3 hPa" but the plots seem to go down to 50hPa. Please clarify.

The caption was incorrect, and has been corrected

- Many of the Figures spell "AURA" rather than "Aura", which is the correct spelling (it is not an acronym), as spelled correctly in most of the manuscript. It would be good to correct the Figures for this.

The spelling has been corrected in the figures.

Also, Fig. 4, Fig. 5, and others in the Supplement have Day/Night Ratio as plot titles, but show ASC/DSC (for Fig. 5) in the axis labels... In reality, day and night during polar summer or winter does not make sense, as it is always either day or night, so it is more correct to state ASC/DSC as what is being calculated, if I am not mistaken. If this is true, the Day/Night labels should more properly be written as ASC/DSC, and for consistency with axis labels... At most latitudes, of course, this is the same thing...

Yes, this is correct, ASC/DSC is the correct wording. We have changed to ASC/DSC throughout the text, or specifically noted what is meant by day and night.

In Fig. 5 (and others like it) there are confusing y-axis tick marks on the right side; it would be best to delete the altitude tick marks there.

This has been corrected in all relevant figures.

Also, in Fig.9, the last sentence could be rewritten a bit as "adjusted to *a* common time of 1:30pm, to coincide with *the* Aura MLS measurement time."

Corrected

Figure S10: change "output" to "outputs" in the last sentence; it would have been nice to indicate what mostly contributes to the differences between the 2017 and 2018 runs (is it geophysical variability in the model, or were there also some sampling differences in how this was calculated ,if matching SAGE sampling patterns?).

We re-worded the last sentence as follows: "The final climatology is the average of output from the SAGE III 2017 and 2018 model runs."

We have added the figure below showing the direct differences between the model simulation in 2017 and 2018 as a function of season and latitude at 4 pressure levels. The difference plotted is the max-min difference in local solar time. However, it is beyond the scope of the manuscript to examine the year to year differences beyond verifying that the year to year variability is small enough that the two can be averaged. There is no sampling difference between the two runs, the model is full spatial sampling.

Model-based Climatology of Diurnal Variability in Stratospheric Ozone as a Data Analysis Tool

Stacey M. Frith¹, Pawan K. Bhartia², Luke D. Oman², Natalya A. Kramarova², Richard D. McPeters², Gordon J. Labow¹

¹Science Systems and Applications, Inc., Lanham, MD, USA

²NASA Goddard Space Flight Center, Greenbelt, MD, USA

Correspondence to: Stacey M. Frith (Stacey.Frith@nasa.gov)

Abstract. Observational studies of stratospheric ozone often involve data from multiple instruments that measure the ozone at different times of day. There has been an increased awareness of the potential impact of the diurnal cycle when interpreting measurements of stratospheric ozone at altitudes in the mid to upper stratosphere. To address this issue, we present a climatological representation of diurnal variations in ozone with a half hour temporal resolution as a function of latitude, pressure and month, based on output from the [Goddard Earth Observing System \(GEOS\) general circulation model coupled to the NASA GEOS-Global Modeling Initiative \(GMI\) chemistry model-run-package \(known as the GEOS-GMI chemistry model\)](#). This climatology can be applied ~~into~~ a wide range of ozone data analyses, including data inter-comparisons, data merging, and analysis of data from a single platform in a non-sun-synchronous orbit. We evaluate the diurnal climatology by comparing mean differences between ozone measurements made at different local solar times to the differences predicted by the diurnal model. The ozone diurnal cycle is a complicated function of latitude, pressure and season, with variations of less than 5% in the tropics and sub-tropics, increasing to more than 15% near the polar ~~summer~~ [boundary day terminator](#) in the upper stratosphere. These results compare well with previous modeling simulations and are supported by similar size variations in satellite observations. We present several example applications of the climatology in currently relevant data studies. We also compare this diurnal climatology to the diurnal signal from a previous iteration of the free-running GEOS Chemistry Climate Model (GEOSCCM) and to the ensemble runs of GEOS-GMI to test the sensitivity of the model diurnal cycle to changes in model formulation and simulated time period.

1 Introduction

Stratospheric ozone has been an environmental concern since the suggestion 45 years ago that anthropogenic chemicals (collectively known as ozone depleting substances; ~~ODS~~ODSs) released into the atmosphere could destroy ozone [Stolarski and Cicerone, 1974; Molina and ~~Rowland~~Rowland, 1974]. Since that time, our understanding of ozone chemistry and dynamics has vastly evolved, and key to that evolution ~~has~~have been high quality satellite and ground-based observations of ozone. These observations were used to quantify ozone loss during the 1980s and early 1990s, and now are being used to quantify the turn around and expected increase in ozone after the ban of many ~~ODS~~ODSs. However, the slow decline in these chemicals, resulting from their long atmospheric lifetimes and the staged reduction of their use through the Montreal Protocol and subsequent amendments, means that the ozone recovery rate will be much slower than the loss rate. Therefore, observations must be sufficiently stable to resolve these small changes in time. Furthermore, measurements from more than one source are required to provide adequate spatial and time coverage to evaluate the full range of effects of ~~ODS~~ODSs on ozone, such that data must be consistent across multiple observation platforms.

Inter-comparison of ozone observations from satellite and ground-based data sources is key to validating independent measurements and maintaining high quality data records. With the need for more stable long-term records, we must consider ever-smaller sources of variability. One such variation is the diurnal cycle in ozone, which had generally been considered small enough to be inconsequential in the middle stratosphere, though the large variations in the upper stratosphere and mesosphere are well known [e.g. Prather, 1981; Pallister and Tuck, 1983]. Although numerous studies have now highlighted observed and modeled peak to peak variations on the order of 5% or more in the middle stratosphere between 30 and 1 hPa [e.g., Sakazaki et al., 2013; Parrish et al., 2014; Schanz et al., 2014a and references therein], adequately resolving the signal on a global scale to account for its effects in data analysis is challenging. Ground-based microwave radiometers have been used to analyze the ozone diurnal cycle ~~in ozone~~ at particular locations from the tropics to the northern hemisphere mid- and high- latitudes [i.e., Ricaud et al., 1991; Conner et al., 1994; Ogawa et al., 1996; Haefele et al., 2008; Palm et al., 2010; Parrish et al., 2014; Studer et al., 2014; Schranz et al., 2018]. Satellite data ~~provides~~provide a more global view of the diurnal cycle. Several satellite missions, including the Upper ~~Atmospheric~~Atmosphere Research Satellite (UARS) Microwave Limb Sounder (MLS), the Superconducting Submillimeter-Wave Limb-

Emission Sounder (SMILES), and the Sounding of the Atmosphere using Broadband Emission Radiometry (SABER) have made measurements from non-sun-synchronous orbits that capture diurnal variations, but it takes more than a month to sample the full diurnal cycle, over which time the ozone has also undergone seasonal and other geophysical changes. Thus, it takes averaging over many years or other statistical techniques to isolate the diurnal variations from other ~~sources~~sources of variability [e.g., Huang et al., 1997; Huang et al., 2010; Sakazaki et al., 2013]. ~~These~~In addition, ~~these~~ missions ~~also~~ do not provide full global coverage.

In this work, we present a climatology of diurnal variability as derived from the NASA Global Modeling and Assimilation Office (GMAO) Goddard Earth Observing System (GEOS) general circulation model coupled to the NASA Global Modeling Initiative (GMI) chemistry package (GEOS-GMI) [e.g., Oman et al., 2013; Orbe et al., 2017]. The model-based climatology provides a global representation of the diurnal cycle as a function of latitude (5° zonal mean), pressure (~ 1 km equivalent altitude vertical resolution) and season (12 months). Parrish et al. [2014] compared the diurnal cycle in a version of this model to that measured by the microwave radiometer at Mauna Loa and found agreement within 1.5% in most cases (see Parrish et al., 2014, Figures 8 and 9). Here we expand on those results, analyzing the model diurnal cycle against available measurements over a range of latitudes. As in the Parrish et al. study, most previous observational studies of the diurnal variability in ozone have included simulations from one or more models to support the observed differences, but we are not aware of a model-based climatology of the global diurnal cycle that is easily accessible for use in wide-ranging data applications. In this work, we do not focus on the chemical and dynamical mechanisms of the ozone diurnal cycle but rather on the validity of the model-derived diurnal climatology as a tool for data analysis. Hereafter we refer to the climatology as GDOC (GEOS-GMI Diurnal Ozone Climatology).

The paper is divided into the following sections: in section 2 we describe the model and the data used in this study; in section 3 we present GDOC and compare its variability to that observed by the SMILES and the UARS and Aura MLS satellite instruments, as well as to that from previously published observational and model-based studies; in section 4 we explore several example uses of GDOC in data analysis; and finally in section 5 we summarize our results, evaluate the robustness of the diurnal signal in multiple model runs, and detail how to access GDOC.

2 Data

2.1 GEOS-GMI Output and the Diurnal Ozone Climatology

The diurnal climatology presented in this work is based on output from the NASA GMAO Version 5 GEOS general circulation model, GEOS-5, [Molod et al., 2015] coupled with the NASA Global Modeling Initiative (GMI) chemistry package [Strahan et al., 2007; Oman et al., 2013; Nielsen et al., 2017], known as GEOS-GMI. Unlike the GEOS Chemistry Climate Model (GEOSCCM) output used in Parrish et al. [2014], which was a free-running model, GEOS-GMI is run in replay mode [Orbe et al., 2017], with dynamics constrained by 3-hourly meteorological fields from the Modern Era Retrospective Analysis for Research and Applications, Version 2 (MERRA-2; Gelaro et al., 2017). The simulation, meant to be concurrent with measurements from the Stratospheric Aerosol and Gas Experiment (SAGE) III instrument aboard the International Space Station (ISS), is currently available from 2017-2018, and will continue as input fields become available.

Model ~~output~~outputs are instantaneous fields, available every 30 minutes on a 1° by 1° latitude by longitude spatial grid. The model is run on 72 pressure levels with a model top at 0.01 hPa, and output is interpolated to so-called Z* pressure levels [~~p~~ $Z^*=1013.25/10^{(z/16)}$ hPa for $z=0,1,2\dots 80$ km] with an approximate pressure-altitude vertical resolution of ~ 1 km (similar to the original model output). Z* pressure levels are often used as a common vertical coordinate when comparing constituent profiles reported (or modeled) on different pressure/altitude surfaces, and is the vertical coordinate used for other climatologies produced by our group (e.g., the McPeters and Labow [2012] and Labow et al. [2015] profile ozone climatologies). We construct the ~~primary~~ climatology by averaging two years of output (2017– 2018) as a function of latitude in 5° bins, pressure, month and time of day (local solar time) every 30 minutes. ~~For~~We first average the model output in latitude to reduce the sampling from 1° to 5°. Then at each fixed longitude, latitude, pressure and day, we interpolate in time (at 30-minute resolution) to convert from UTC to local solar time for that longitude. Note that we sample model output from three consecutive days (in UTC) to get a full local solar time diurnal cycle at each longitude. We then average the diurnal cycles at each longitude to get a daily zonal mean diurnal cycle, and then we average over available days for each month. Finally, for each latitude, level and month, the half-hourly climatological values are normalized to the value at midnight (11:45-00:15 local time bin) and the final

climatology is expressed in terms of variation from midnight. We note that GDOC can be re-normalized to any reference time as is most appropriate for a given analysis.

Uncertainty estimates for GDOC should be based on the standard error of the mean of the model output averaged to construct the climatology. However, with each bin containing 108,000 data points (360 longitude x 5 latitude x 60 days), the standard error of the mean is unrealistically low. The model ozone fields are spatially and temporally correlated, so the true number of independent data points is much lower. To estimate the actual number of independent data points we compute longitudinally lagged correlations at each grid point in a given day and assume that the data points are independent when the lagged correlation drops below a threshold value. Based on this analysis (see Figure S1 and corresponding discussion) we found that there are ~ 12 independent measurements in each daily bin (~ sampling of 30° longitude). Output in each 5° latitude band is also considered to be correlated. Thus, we use $n=720$ ($12 * 60$ days) for all computations of GDOC standard error of the mean.

We also use output from the free-running GEOSCCM simulation as presented in Parrish et al. [2014] and from a previous iteration of GEOS-GMI to test the robustness of GDOC to changes in the model formulation (including updates to the input photochemistry and reaction rates) and to different simulation years. Test climatologies from the additional model simulations are representative of different years but are constructed in the same manner. ~~Supplemental Figure S10 shows an example of the diurnal climatologies constructed from four separate simulations. The overall patterns from all the simulations are very similar, suggesting the representation of the diurnal cycle within the model is well established.~~

2.2 Ozone Observations

We use ozone observations from multiple data sources to test GDOC in a variety of circumstances. Specifically, we use data from MLS instruments aboard the NASA UARS and Earth Observing Satellite (EOS) Aura platforms; the second generation Solar Backscatter Ultraviolet (SBUV/2) series of instruments since 2000, which include those launched on NOAA satellites 16, 17, 18, and 19; the Ozone Monitoring Profiler Suite (OMPS) Limb Profiler (LP) and Nadir Profiler (NP)

instruments aboard the NASA/NOAA Suomi National Polar-orbiting Partnership (S-NPP) satellite; the SMILES instrument which made measurements from the ISS and the SAGE III instrument currently aboard the ISS (hereafter SAGE III/ISS). Table 1 shows the salient characteristics of the data sets used in this analysis and appropriate references for more information on each instrument.

All high vertical resolution data records except SAGE III/ISS and OMPS LP are reported in pressure coordinates, and are first interpolated to Z^* pressure levels. SAGE III/ISS and OMPS LP data are reported in altitude coordinates, and MERRA-2 dynamical fields are used to convert between geometric altitude and pressure. OMPS NP and SBUV report ozone as partial column densities (in DU) in pressure layers. Number density and mixing ratio profiles are integrated to give cumulative column densities with pressure, which can be interpolated to re-partition the partial columns to match the SBUV/OMPS NP broad vertical sampling. Monthly climatological averages of satellite data are constructed (with the exception of SMILES and SAGE III/ISS, which are averaged over the entire available time period) in 5° latitude bins. UARS MLS and SMILES are additionally averaged into one-hour time bins. An estimated seasonal cycle is removed from the nine months of SMILES data as outlined in Sakazaki et al. [2013, Figure 3] and the data are not binned by month. Though UARS MLS also samples the diurnal cycle over an extended period, the geophysical variability is largely removed in the 9-year average by month and the error bars capture the remaining variability. In this work, we use UARS MLS data for qualitative comparisons only, and thus do not apply a more rigorous analysis to isolate the diurnal cycle.

3 Evaluation of Diurnal Climatology

3.1 Characterization of the Diurnal Cycle in GDOC

We first show several examples of GDOC, highlight some of the salient features, and compare generally to past studies. Figure 1 shows GDOC, normalized to the value at midnight, as a function of hour of day and pressure for four latitude bands and months. The ratio is shown with a contour interval of 0.025 (2.5%). The first panel (upper left) shows the climatology for March at $15\text{--}20^\circ$ N. Here the most obvious feature is the low ozone during the day in the lower mesosphere, the well-known mesospheric ozone diurnal cycle [e.g. Pallister and Tuck, 1983]. There is very little,

if any variation in the nighttime values at these altitudes. Below 1 hPa, there are variations at the sub-5% level. Unlike at higher levels, near 2 hPa the diurnal ozone nighttime values decrease by 2.5% between midnight and dawn, and then vary up and down during the day (see also Figure 2). Results in this latitude band correspond to previous results shown in Parrish et al. [2014], comparing an earlier version of the model to diurnal variations derived from the microwave radiometer at Mauna Loa. Overall, that study showed differences between model and data generally within 1-1.5%. The largest discrepancy was noted in the pre-dawn hours near 2 hPa, where the microwave instrument showed increasing rather than decreasing ozone. However, ~~data from the~~ SMILES ~~satellite~~ data also suggest the ozone is decreasing over this period (Figure 2; Parrish et al., Figure 10). ~~Supplemental~~ Figure S1S2 (top panels) show GDOC at 15-20° N for the additional months of January and June. The pre-dawn diurnal ozone decrease is larger in January, as was seen by Parrish et al.

The second panel (upper right) shows results for January at 45-50°N, which can be directly compared to a diurnal climatology developed from the GROMOS microwave radiometer in Bern, Switzerland [Studer et al., 2014, Figure 4a], as well as collocated model output from the Whole Atmosphere Community Climate Model (WACCM) and the Hamburg Model of Neutral and Ionized Atmosphere (HAMMONIA) used in the same study. Compared to the March subtropical climatology in the first panel, the shorter period of daylight hours is evident in the higher latitude January output. GDOC shows a loss of just over 20% at 0.3 hPa, which is somewhat less than that shown by GROMOS or the WACCM and HAMMONIA models, which are closer to 25%. Below about 1.5 hPa, the pattern shifts from daytime low ozone to a pattern of lower ozone in the morning and higher ozone in the afternoon, with variations of ~~greater~~ more than 5%. GROMOS and the collocated models show a similar shift, though at slightly different altitudes. GDOC agrees more closely with the model output from the GROMOS study, and the authors suggest that the limited vertical resolution of the microwave data might be the cause of the discrepancy [Studer et al., 2014]. This characteristic pattern with higher afternoon ozone in the upper stratosphere diurnal cycle has been widely reported in other observations from ground-based and satellite data [e.g., Haefele et al., 2008, Huang et al., 2008; Sakazaki et al., 2013, Parrish et al., 2014, Schranz et al., 2018]. Using the WACCM model, Schanz et al. [2014a] present a detailed breakdown of the photochemical reactions that contribute to the mid-latitude ozone diurnal cycle at 5 hPa (see also

Haefele et al., 2008). ~~Supplemental~~Figure ~~S2S3~~ shows the seasonal variability of GDOC at 45-50°N at several altitudes, which matches the higher summertime amplitude model diurnal cycle reported ~~in summer~~ by Studer et al. [2014] and Schanz et al. [2014a].

The lower two panels of Fig. 1 show the diurnal cycle in the northern hemisphere polar summer. The diurnal variability in both the mesosphere and stratosphere is largest near the Arctic Circle (lower left) and decreases nearer the pole (lower right). Near the polar day boundary, the diurnal cycle varies by greatermore than 15% in the stratosphere. This large signal was reported in WACCM output by Schanz et al. [2014a; 2014b]. Recently, one year of microwave radiometer data taken at Ny-Alesund, Spitsbergen, Norway (79° N) showed similar variability with a June peak to peak variation of 5% at 1 hPa (night time ozone higher) and similar amplitude variations but with larger afternoon values higher at 3 hPa [Schranz et al., 2018]. The authors also included co-located WACCM model results in their analysis, which compared well with the data after accounting for the reduced vertical resolution of the microwave instrument. The high-resolution WACCM output variations are 10% at 1 hPa and 8% at 3 hPa, in very close agreement with the GDOC signal at 75-80° S. ~~Supplemental~~Figure ~~S1S2~~ (bottom panels) shows the summer polar diurnal cycle in the Southern Hemisphere, which is nearly perfectly symmetric with that in the North.

Figure 2 shows GDOC at 65-70° N as a function of time of day at four pressure levels. Climatological values in March, June, September and December demonstrate the marked variation in the diurnal cycle with season at high latitudes. The summertime (June) diurnal cycle is the largest at all pressure levels. At 0.5 hPa, the square-wave pattern dominates for all seasons, though it is weak in the winter. In the summer, the mesospheric diurnal pattern persists to 1 hPa, while other seasons show a more complicated pattern, with the equinox months showing a secondary peak in the late afternoon. At 3 and 5 hPa, all months except December show an early morning minimum and afternoon maximum. The December diurnal variability is confined to the hours around noon due to limited exposure to sunlight near the polar night boundary. The uncertainty is also greatest in December (winter) at all levels.

A more detailed depiction of the GDOC uncertainty is given in Figure 3. Here we show the uncertainty at noon local solar time (in percent) as a function of month and latitude on four pressure levels. The uncertainties are very consistent in local solar time, so the noon results are representative of all times. The uncertainties (as defined by the standard error of the mean) are mostly less than 1%. Uncertainties of 1% or greater are highlighted in red, occurring at high latitudes in the winter season of each hemisphere. The largest uncertainties are ~ 2%.

3.2 Diurnally-Resolved Satellite Data

In Figure 34, we directly compare the general features of GDOC at several pressure levels to those derived from diurnally resolved data from UARS MLS and SMILES satellite-based measurements as well as Aura MLS averages at 1:30am and 1:30pm (black symbols and vertical dotted lines). Specifically, we plot ozone variability as a function of hour of day normalized to the mean daily value for each product. The satellite data tend to be noisy, so we normalize to the daily mean rather than to values at a specific time. Because of their orbital characteristics, both UARS MLS and SMILES have their best coverage within ~ 30° of the equator, so we limit our comparisons to low latitudes. We show results at 15-25°N in Figure 24, but other latitude bands in the tropics are similar. This comparison is qualitative in that we compare the zonal means and we do not attempt to isolate the diurnal cycle in the UARS MLS record beyond simply averaging the data over many years. The deseasonalized SMILES data as derived in Sakazaki et al. [2013] were provided by the authors [T. Sakazaki, personal communication, 2014]. Although the satellite data are noisy from hour to hour, the overall daily variability is accurately represented by GDOC. At 0.5 hPa the mesospheric diurnal pattern prevails, and GDOC captures the amplitude of the day to night ozone differences measured by the satellite ~~data~~instruments. At 1.5 hPa, the pattern is a hybrid of the mesospheric and stratospheric diurnal cycle, with two relative ~~maximums~~maxima in the early morning and late afternoon, seen also in the SMILES data and to some degree by UARS MLS. Finally at 5 hPa the stratospheric pattern dominates, with measurements and climatology showing ~~a relative high ozone value~~the highest daily values in the mid-afternoon. The satellite data agree within ~ 4% on the amplitude of the signal, with GDOC roughly reflecting the average of the satellite data.

3.3 Ascending/Descending (Day-/Night) Differences

We complete a more rigorous investigation of GDOC by analyzing ~~the day-night differences~~ in how well the model ~~relative to the day-night~~ reproduces ascending-descending differences in the Aura MLS record. At the equator, Aura MLS makes measurements at 1:30 pm and 1:30 am local solar time, but at other latitudes the exact measurement time varies due to the orbit inclination. Outside of polar latitudes, the ascending measurement is made during daylight hours while the descending measurement is made at night. Hereafter we refer to “day” and “night” rather than ascending and descending. Profiles from GDOC are selected to match the location and measurement local solar time of each MLS profile, and then averaged for direct comparison with MLS day and night averages. For this comparison, when selecting the climatological profiles, we interpolate in time but not in latitude. Figure 45 shows the ratio of ~~the daytime average to the nighttime average~~ averages as measured by Aura MLS (top panels) and represented by corresponding profiles from GDOC- (bottom panels) as a function of latitude and pressure for two months, June and December.

The day to night ratio in the upper stratosphere, above ~ 1.5 hPa, shows the typical mesospheric diurnal pattern of low ozone in the daytime and high ozone at night [i.e., Pallister and Tuck, 1983]. Below this level the daytime ozone is higher than the nighttime value, but the pattern varies with latitude. As expected, there is little variation between day and night values at high latitudes in polar night [see also Schranz et al., 2018]. In polar day, however, there is a variation of greater than 20% between 5 and 1 hPa near 70° N. Overall GDOC closely matches the spatial pattern and amplitude of ~~that in the MLS with~~ the ratios measured by MLS, with agreement generally ~~in agreement~~ to within 2%. In the tropics near 1 hPa, we note a local ~~minimum~~ minimum in the day to night ozone ratio in the Aura MLS data. GDOC also shows a local ~~minimum~~ minimum, but the amplitude of this feature is not as pronounced as in the data. It is interesting to note the similarities in the pattern of the diurnal cycle below 30 hPa. However, we do not validate GDOC below 30 hPa because the diurnal variability is small and does not need to be accounted for at these levels.

Figure 56 shows profiles of the day to night ratio from the model and from Aura MLS at 65-70° N and 65-70° S for the months of March, June, September and December. The error bars indicate twice the standard deviation of the Aura MLS profiles averaged from 2004-2018. We show the

standard deviation to highlight the interannual variability of the ratio as measured by Aura MLS. In this case the ratio of the GDOC profiles in the given latitude bin at the ascending and descending time is shown (i.e. GDOC is not explicitly sub-sampled to each MLS profile) and the error bar is twice the root mean square of the two corresponding uncertainty profiles. Though there are some differences between the model simulations and observations, most notably the small shift in altitude in the June signal at 65-70° N and the offset above 2 hPa in September at 65-70° S, for the most part GDOC reliably reproduces the signal in the observations within 2-percent% or better. Additional profile comparisons of the day to night ratio from GDOC and Aura MLS can be found in Supplemental Figures S3-S8S4-S9.

4 Example Diurnal Climatology Applications

4.1 SAGE III/ISS Sunrise Sunset Comparisons

SAGE III/ISS infers ozone profiles by measuring solar irradiance that has passed through the atmosphere during local sunrise and sunset events. One approach to evaluating these data is by checking the consistency of the measured sunrise and sunset profiles, but care must be taken to account for real diurnal differences between sunrise and sunset. Sakazaki et al. [2015] presented a thorough study of sunrise-sunset differences from occultation instruments SAGE II, UARS HALOE and ACE-FTS in the tropics between 10° N and 10° S. Their analysis included output from the WACCM Specified Dynamics chemical transport model, and both observations and model indicated an asymmetry between sunrise and sunset measurements in the tropics, with sunrise satellite measurements being larger than those at sunset below ~30 km and above ~55 km. Figure 67 shows the ~~estimated~~ ratio of mean (2017-2018) SAGE III/ISS sunrise values to sunset values (SR/SS; red) and that computed from GDOC sub-sampled to match the SAGE III/ISS measurements (blue). Results are shown in three broad latitude bands, and the SAGE III/ISS profiles have been interpolated to pressure levels in this comparison (using MERRA-2 temperature/pressure data) in this comparison. The SAGE error bars denote twice the standard error of the mean (sem), computed as the root mean square of the sunrise and sunset sem values. The blue error bars for GDOC indicate the variability of the SAGE-sampled reconstructions (computed in the same way as the SAGE error bars). The overlaid orange error bars (roughly the width of the plotting symbol) represents the model uncertainty, computed as the root mean square

of the model standard deviation profiles at SAGE sampling, divided by the square root of n ($=720$). Note that the spatial-temporal sampling of profiles is different in the sunrise and sunset averages. By matching the diurnal climatology to each profile, we can represent the impact of the sampling on the ~~diurnal cycle~~, but other geophysical variability that the climatology cannot reproduce may contribute to the measured differences. The SR/SS pattern from GDOC is similar to that reported in Sakazaki et al. [2015] with sunrise profiles greater than sunset profiles (ratio > 1) below ~ 15 hPa (~ 30 km) and above ~ 0.7 hPa (~ 51 km) in the tropics (middle panel). We note that GDOC indicates SR/SS > 1 occurs at 51 km, which is somewhat lower than reported by Sakazaki et al. [2015] in observations (~ 55 km) and WACCM model results (~ 53 km). At ~~middle-mid-~~latitudes, the GDOC sunrise/sunset differences are smaller (SR/SS is closer to 1), compared to the tropics, with little difference below 15 hPa and a smaller difference in the upper stratosphere. The GDOC SR/SS pattern is also shifted downward by a few kilometers in the ~~middle-mid-~~latitudes. The SAGE III/ISS SR/SS ratio generally follows the pattern indicated by GDOC, and is within $\sim 1\%$ of the GDOC ratio below 2 hPa. Above 2 hPa GDOC and SAGE III/ISS diverge. At these levels ~~the influence of the diurnal cycle on,~~ the SAGE III/ISS ~~measurement is difficult to model because of retrieval does not account for~~ the sharp diurnal gradient in the ozone along the line of ~~sightsight~~ of the instrument. However, GDOC representations near the terminator may also be biased due to smearing of the diurnal ozone gradient in the monthly average as the terminator time shifts within the month. Also, as noted above, there is some variation between GDOC, WACCM and observations in the SR/SS pattern in the tropics. Nevertheless, these differences suggest potential discrepancies between SAGE III/ISS sunrise and sunset measurements that are currently being explored (R. Damadeo, personal communication, 2019). The purpose of this work is not to evaluate SAGE III/ISS observations but to demonstrate how GDOC can be used in such evaluations.

4.2 SAGE III/ISS Comparisons with Other Instruments

As with SAGE III/ISS internal sunrise/sunset comparisons, when evaluating the data relative to independent measurements, the local solar time of the measurements should be taken into account. Occultation instruments measure at local sunrise and sunset while limb and nadir measurements are taken at various times throughout the day, depending on the instrument (see Table 1). In this example, we compare SAGE III/ISS sunrise and sunset profiles to co-located profiles from Aura

MLS, OMPS Limb Profiler (OMPS LP) and OMPS Nadir Profiler (OMPS NP). Both OMPS (LP and NP) and Aura MLS measure at or near 1:30 pm local solar time. In the case of Aura MLS and OMPS LP, co-located profiles are defined as the nearest profile (within 1000 km) to the SAGE III/ISS profile, on the same day, and comparisons are done in altitude. ~~For OMPS NP co-located Aura MLS profiles are the distance-weighted average of all profiles occurring within 1000 km of the SAGE profile on the same day and comparisons are converted from volume mixing ratio on pressure levels.~~ surfaces to number density on altitude surfaces using co-located MERRA-2 temperature and pressure data. Figure ~~7~~8 shows mean differences in the 20° - 60° N latitude band between SAGE III/ISS profiles (sunrise and sunset) relative to OMPS LP (upper panel) and Aura MLS (lower panel) before (red) and after (blue) using the diurnal climatology to ‘adjust’ the SAGE III/ISS profiles to the equivalent measurement time of the correlative data set. Again, our intention is not to do a thorough analysis of the differences but to highlight the influence of the diurnal cycle ~~when completing on~~ such analyses. Near 50 km, the mean differences are reduced by 5% or more when accounting for the diurnal cycle. Similarly, differences are reduced below 44 km, with SAGE III/ISS coming into very good agreement with Aura MLS at these altitudes.

Figure ~~8~~9 shows comparisons between SAGE III/ISS and OMPS NP profiles in three latitude bands. While OMPS LP is a limb scatter instrument that measures at high vertical resolution, OMPS NP is a nadir backscatter measurement with a broad vertical resolution in the stratosphere. ~~The Higher resolution instrument measurements (SAGE III/ISS profiles, MLS, OMPS LP) are first often used to help evaluate the lower resolution nadir instruments. This is critical to ensure OMPS NP can continue the 40+ year record of trend quality ozone from the SBUV series of nadir instruments. OMPS NP returns partial column ozone amounts (DU) in pressure layers. Before the SAGE III/ISS sunrise and sunset profiles are averaged, the number density profiles are integrated vertically, giving column densities that are converted to DU and repartitioned into layers that match the OMPS NP vertical resolution.~~ before the sunrise and sunset profiles are averaged. In this case, co-located profiles are the distance-weighted average of all profiles occurring within 1000 km of the SAGE profile on the same day and comparisons are on pressure levels. The top panel shows the mean differences for sunrise-only (yellow) and sunset-only (purple) profiles. The bottom panel shows the same differences after the SAGE III/ISS profiles are converted using GDOC to an equivalent time of 1:30 pm to match the time of the OMPS NP measurements. Note

that this comparison is focused lower in the stratosphere than in the previous figure. As such, the diurnal impacts are smaller. The largest changes are in the 1.0-1.6 and 1.6-2.5 hPa layers, though there are impacts at the 1-2% level in the 6-10 hPa layer and even lower in the tropics. After the diurnal adjustment, the sunrise and sunset biases are closer, and both indicate a shift in the bias above ~ 10 hPa. The remaining pattern of differences is consistent with ~~the known bias pattern~~ biases previously reported in the nadir UV backscatter series of instruments relative to satellite (SAGE II, UARS and Aura MLS) and ground-based (select microwave and lidar) data [i.e. Kramarova et al., 2013; Frith et al., 2017]. Namely, the nadir backscatter instruments tend to have a negative bias below 10 hPa and above 2.5 hPa, and a positive bias near 7 hPa. These examples illustrate how accounting for the diurnal cycle can help to both ascertain the true differences in the profiles and reduce noise in the inter-comparisons.

4.3 Merging SBUV Ozone Records

Representing the diurnal cycle is also important when merging multiple ozone data sets to construct a single long-term consistent data record. In this example we consider the SBUV series of nadir-view backscatter instruments, which is used to construct the Merged Ozone Data (MOD) record [Frith et al., 2014; Frith et al. 2017]. The SBUV/2 instruments on NOAA satellites were launched into drifting orbits such that the measurement time slowly changed over years. In addition, NOAA-17 SBUV/2 was launched into a late morning orbit, while the others were in early afternoon orbits, contributing to differences of several hours in overlapping measurements between instruments. Similarly, NOAA-16, though launched into an afternoon orbit, drifted such that measurements after 2012 were made in the early morning.

The combination of morning and afternoon orbits and drifting orbits can impart diurnally induced bias, drift and seasonal-scale variation between the SBUV/2 data records. We investigate this by comparing NOAA-16, -17 -18 and -19 to Aura MLS volume mixing ratio profiles are integrated to give column density profiles (converted to DU) which are then repartitioned to match the vertical sampling of the SBUV/2 data. Figure 910 shows the 4-6.4 hPa layer ozone difference time series at 10-15° S. The top panel shows the original differences between each SBUV/2 instrument and Aura MLS, and the bottom panel shows the differences after each SBUV measurement has been adjusted using GDOC to the Aura measurement time.

Aura MLS is used as a transfer standard and does not change. Here the primary impact of the diurnal cycle correction is to reduce the bias between the instruments. At the same latitude band but in the 2.5-4-hPa layer, shown in Figure ~~40~~11, there are clear drifts over portions of the SBUV records relative to MLS that are largely removed after accounting for the diurnal cycle. Though in this case relative biases between the instruments remain, accounting for a consistent bias in a merged record is much easier than accounting for short-term drifts. Finally, Figure ~~41~~12 shows the effect of the seasonal variation in the diurnal cycle at higher latitudes (see Figure 45 and Figure ~~S2~~S3). Here the SBUV instruments all show a seasonal cycle relative to Aura MLS, but after adjusting for the diurnal cycle the individual SBUV instrument seasonal cycles are in much better agreement relative to MLS. These varied effects can be understood by considering the diurnal cycle in each example, as shown in ~~Supplemental~~ Figure ~~S9~~S10. The SBUV/2 records shown in Figures ~~9-11~~10-12 vary in measurement time from 2 to 4 pm and from 8 to 10 am. At 10-15° S at 5 hPa there is a difference in the diurnal cycle from morning to afternoon, but little change between 8 and 10 am or between 2 and 4 pm. However at 3 hPa there is a continuous gradient in ozone as a function of hour from 8 am to 4 pm. Thus, there is not only a bias between morning and afternoon measurements, but also a drift is induced as SBUV measurements shift earlier or later in time between the hours of 8 to 10 am and 2 to 4 pm. Finally, at 50-55°S at 7 hPa there is no diurnal signal in June-July-August but there is a 5% variation between morning and afternoon ozone in December-January-February, leading to diurnally induced seasonal differences between instruments.

5 Summary and Conclusions

In this paper, we present a global climatology of the ozone diurnal cycle based on the NASA GEOS-GMI chemistry model. The climatology provides ozone ~~levels~~values every 30 minutes during the day, expressed as ~~the ratio of ratios to~~ the value at midnight. (though it can be renormalized relative to other times). It varies as a function of latitude, pressure, and month, with a latitude resolution of 5° and a vertical resolution of ~ 1 km equivalent pressure altitude. Previous studies of diurnal ozone observations often include co-located model results for comparison, but as far as the authors are aware, this is the first easily accessible model-based climatology to be made available for general data analysis purposes. A model-based climatology is useful because no observational data source provides a full representation of the ozone diurnal cycle. However,

this fact also makes the model output difficult to validate. Here we compare the climatology to time-resolved satellite-based data from UARS MLS and SMILES, and compare the day to night climatological ratios to those derived from Aura MLS measurements. We also compare the climatology to previously published results including model analyses and diurnally resolved data from ground-based microwave radiometers. The GEOS-GMI diurnal climatology compares well with all sources; the most quantitative comparison against Aura MLS daytime to nighttime profiles ratios shows agreement typically within 2%.

The diurnal climatology ~~depictsexhibits~~ the largest variability during summer near the polar day boundary (65-70°), as reported previously by Schanz et al. [2014a, 2014b] based on WACCM model output. This is also supported by ratios of daytime to nighttime ozone profiles from Aura MLS. The hourly ozone variation ~~transitionsshifts~~ from a mesospheric pattern of low ozone during the day and high ozone at night to a stratospheric pattern of low ozone in the morning and high ozone in the afternoon. However, the amplitude of the signals and the altitude of the transition vary significantly with season, leading to very complicated diurnal patterns that are not easily characterized in data inter-comparisons.

In this work, we do not focus on the chemical and dynamical mechanisms of the diurnal cycle but rather on the validity of the model-derived diurnal climatology as a tool for data analysis. We present a series of examples that ~~highlighthighlights~~ the usefulness of the climatology in data analysis as well as ~~demonstratedemonstrates~~ the consistency between the observed and predicted ozone variations. ~~In an additional test of~~We represent the robustnessuncertainty of the climatological mean values as two times the standard error of the mean of the bin averages, assuming n=720 independent measurements in each bin. This gives error bars that are 2% or less.

The comparisons presented here give us confidence in the climatology, but we also need to consider potential sources of uncertainty. Systematic changes in the diurnal cycle over a month or year-to-year will be smoothed within the climatology. The Aura MLS ASC/DSC ratios (Figures 6 and S4-9) do not suggest significant interannual variability in the large-scale diurnal structure. To further quantify this, we compare GDOC derived using just 2017 model, we considered output to that derived using just 2018 model output, as shown in Figure S11. Below 5 hPa the differences

are generally less than 1%. At higher levels, there are sporadic instances of larger differences (3-5%) in the tropics and at higher latitudes but overall, differences remain small. As more years of model output become available, we will be able to better characterize interannual variability in the model. Similarly, true day-to-day or longitudinal variability in the diurnal cycle will be smoothed out in the zonal average over the month. We find varying degrees of both day-to-day and longitudinal variability in the model diurnal cycles, and this is a subject of ongoing analysis, but characterizing these sources of variability is beyond the scope of this manuscript. Care should be taken when reconstructing daily values using the monthly GDOC, especially near the terminator in the upper stratosphere, where the ozone gradient is sharp and varies in time over the month.

A final source of uncertainty is potential model error. The climatology is normalized, so the only relevant error is representation of the diurnal cycle. To further test the stability of the model diurnal cycle, we consider several different simulations using iterative versions of the model and/or simulations of different years, and ~~compared~~compare the diurnal cycle derived from each simulation. ~~Supplemental~~Figure S10S12 shows the December day-night ratios from diurnal climatologies constructed from four separate simulations. The overall patterns from all the simulations are very similar, suggesting that the representation of the diurnal cycle within the model is well established. This does not preclude a model issue that is present in all model versions. Ideally, as the model is used more in data analyses, such studies will also provide feedback to the modeling team.

We recommend using GDOC primarily for monthly zonal mean analyses in the pressure range from 30 to 0.3 hPa. Comparisons against the various satellite measurements presented in this study suggest that the climatology captures diurnal variations to well within 5% in most cases. For applications that require accurate knowledge of high temporal and spatial resolution changes in ozone we advise using the original model output (see *Data Availability*).

Data Availability.

The GEOS-GMI diurnal ozone climatology is stored as a NetCDF file and is available for download on our local NASA Goddard Code 614 TOMS access site <https://acd->

[ext.gsfc.nasa.gov/anonftp/toms/https://acd-ext.gsfc.nasa.gov/anonftp/toms/GDOC_diurnal/](https://acd-ext.gsfc.nasa.gov/anonftp/toms/https://acd-ext.gsfc.nasa.gov/anonftp/toms/GDOC_diurnal/) (last access ~~August 20, 2019~~[February 19, 2020](https://acd-ext.gsfc.nasa.gov/anonftp/toms/GDOC_diurnal/)) under subdirectory ~~GEOS-GMI_Diurnal_Climatology~~[GDOC_diurnal](https://acd-ext.gsfc.nasa.gov/anonftp/toms/GDOC_diurnal/). Also available from this site are the SBUV/2 data (subdirectory sbuv) and OMPS NP data (subdirectory omps_np). These data are also accessible via links from the Merged Ozone Dataset (MOD) website at https://acd-ext.gsfc.nasa.gov/Data_services/merged/instruments.html (last access ~~August 20, 2019~~[February 19, 2020](https://acd-ext.gsfc.nasa.gov/Data_services/merged/instruments.html)). OMPS LP and NP data and UARS and Aura MLS data are archived at the NASA Goddard Earth Sciences Data and Information Services Center (GES-DISC) (<https://disc.gsfc.nasa.gov>, last access August 20, 2019). SAGE III/ISS are available at the NASA Langley Atmospheric Science Data Center (ASDC) (https://eosweb.larc.nasa.gov/project/sageiii-iss/sageiii-iss_table, last access August 20, 2019). SMILES data are available from the Data Archives and Transmission System (DARTS) (<http://darts.jaxa.jp/stp/smiles/>, last access August 20, 2019). The Mauna Loa hourly resolved microwave data are available by request (A. Parrish, parrish@astro.umass.edu). Additional model output from the current GEOS-GMI simulation is available for collaborators by request (L. D. Oman, luke.d.oman@nasa.gov).

Author Contributions.

S. M. Frith conducted the primary analysis including constructing the GEOS-GMI diurnal ozone climatology and applying the climatology to various data analysis tasks. L. D. Oman formulated and ran the model simulations and provided guidance interpreting the model output. N. A. Kramarova provided analysis of OMPS LP and SAGE III/ISS data. G. J. Labow contributed to Aura MLS and SBUV measurement analysis. P.K. Bhartia conceived the original idea for this

work and oversaw its development, and R. D. McPeters provided funding support and project management. S. M. Frith prepared the manuscript with significant contributions from all authors.

Competing Interests.

The authors declare that they have no conflict of interest.

Acknowledgements.

S. M. Frith is supported under NASA WBS 479717 (Long Term Measurement of Ozone). Model simulations are supported by the SAGE III/ISS Science Team and NASA MAP programs and the high-performance computing resources were provided by the NASA Center for Climate Simulation (NCCS). The authors thank R. Stolarski for his helpful comments on the manuscript. We also thank the various instrument teams for providing the data used in this study, particularly those responsible for SAGE III/ISS, Aura MLS, OMPS and SBUV.

References

- Bhartia, P. K., McPeters, R. D., Flynn, L. E., Taylor, S., Kramarova, N. A., Frith, S., Fisher, B., and DeLand, M.: Solar Backscatter UV (SBUV) total ozone and profile algorithm, *Atmos. Meas. Tech.*, 6, 2533–2548, doi:10.5194/amt-6-2533-2013, 2013.
- Chu, W. and Veiga, R.: SAGE III/EOS, *Proc. SPIE*, 3501, 52–60, doi:10.1117/12.577943, 1998.
- Connor, B. J., Siskind, D. E., Tsou, J. J., Parrish, A., and Rems-berg, E. E.: Ground-based microwave observations of ozone in the upper stratosphere and mesosphere, *J. Geophys. Res.*, 99, 16757–16770, doi:10.1029/94JD01153, 1994.
- Frith, S. M., Stolarski, R. S., Kramarova, N. A., and McPeters, R. D.: Estimating uncertainties in the SBUV Version 8.6 merged profile ozone data set, *Atmos. Chem. Phys.*, 17, 14695–14707, doi:10.5194/acp-17-14695-2017, 2017.

- Frith, S. M., Kramarova, N. A., Stolarski, R. S., McPeters, R. D., Bhartia, P. K., and Labow, G. J.: Recent changes in total column ozone based on the SBUV Version 8.6 Merged Ozone Data Set, *J. Geophys. Res. Atmos.*, 119, 9735–9751, doi:10.1002/2014JD021889, 2014.
- Froidevaux, L., Jiang, Y. B., Lambert, A., Livesey, N. J., Read, W. G., Waters, J. W., Browell, E. V., Hair, J. W., Avery, M. A., McGee, T. J., Twigg, L. W., Sumnicht, G. K., Jucks, K. W., Margitan, J. J., Sen, B., Stachnik, R. A., Toon, G. C., Bernath, P. F., Boone, C. D., Walker, K. A., Filipiak, M. J., Harwood, R. S., Fuller, R. A., Manney, G. L., Schwartz, M. J., Daffer, W. H., Drouin, B. J., Cofield, R. E., Cuddy, D. T., Jarnot, R. F., Knosp, B. W., Perun, V. S., Snyder, W. V., Stek, P. C., Thurstans, R. P., and Wagner, P. A.: Validation of Aura Microwave Limb Sounder stratospheric ozone measurements, *J. Geophys. Res.*, 113, D15S20, doi:10.1029/2007JD008771, 2008.
- Gelaro, R., McCarty, W., Suárez, M. J., Todling, R., Molod, A., Takacs, L., Randles, C. A., Darmenov, A., Bosilovich, M. G., Reichle, R., Wargan, K., Coy, L., Cullather, R., Draper, C., Akella, S., Buchard, V., Conaty, A., da Silva, A. M., Gu, W., Kim, G., Koster, R., Lucchesi, R., Merkova, D., Nielsen, J. E., Partyka, G., Pawson, S., Putman, W., Rienecker, M., Schubert, S. D., Sienkiewicz, M., and Zhao, B.: The Modern-Era Retrospective Analysis for Research and Applications, Version 2 (MERRA-2). *J. Climate*, **30**, 5419–5454, doi:10.1175/JCLI-D-16-0758.1, 2017.
- Haefele, A., Hocke, K., Kämpfer, N., Keckhut, P., Marchand, M., Bekki, S., Morel, B., Egorova, T., and Rozanov, E.: Diurnal changes in middle atmospheric H₂O and O₃: observations in the Alpine region and climate models, *J. Geophys. Res.*, 113, D17303, doi:10.1029/2008JD009892, 2008.
- Huang, F. T., Reber, C. A., and Austin, J.: Ozone diurnal variations observed by UARS and their model simulation, *J. Geophys. Res.*, 102, 12971–12985, doi:10.1029/97JD00461, 1997.
- Huang, F. T., Mayr, H. G., Russell, J. M. I., and Mlynczak, M. G.: Ozone diurnal variations in the stratosphere and lower mesosphere, based on measurements from SABER on TIMED, *J. Geophys. Res.*, 115, D24308, doi:10.1029/2010JD014484, 2010.
- Kasai, Y., Sagawa, H., Kreyling, D., Dupuy, E., Baron, P., Mendrok, J., Suzuki, K., Sato, T. O., Nishibori, T., Mizobuchi, S., Kikuchi, K., Manabe, T., Ozeki, H., Sugita, T., Fujiwara, M., Irimajiri, Y., Walker, K. A., Bernath, P. F., Boone, C., Stiller, G., von Clarmann, T., Orphal, J., Urban, J., Murtagh, D., Llewellyn, E. J., Degenstein, D., Bourassa, A. E., Lloyd, N. D.,

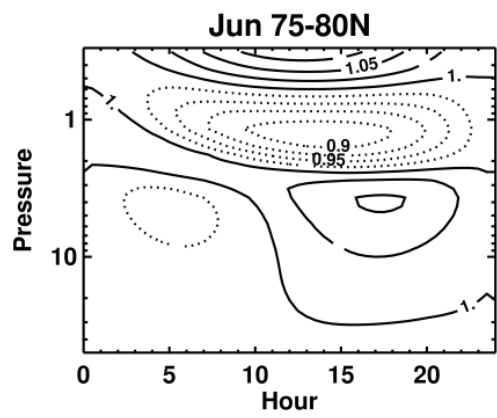
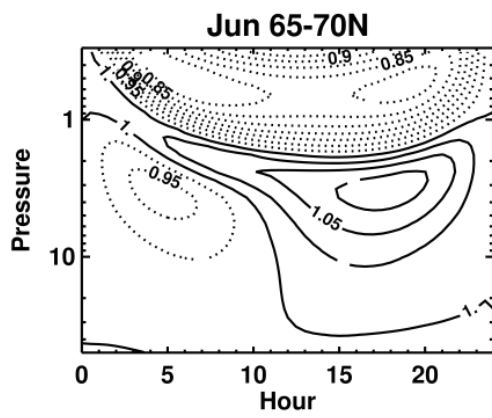
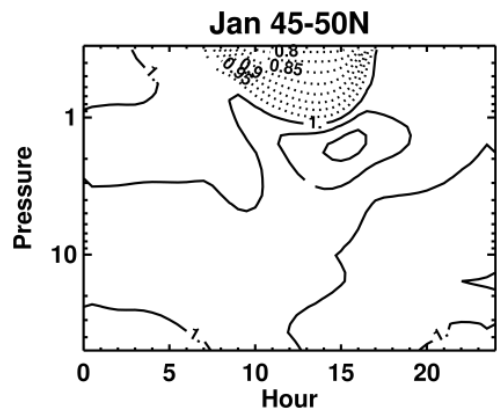
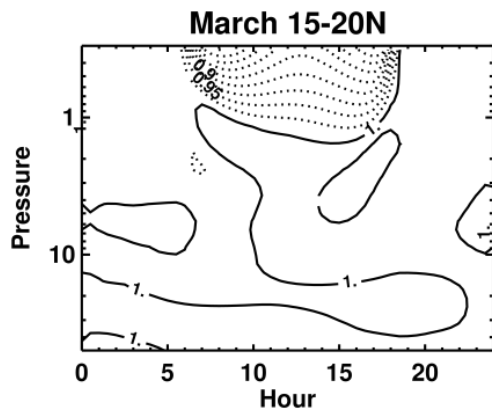
- Froidevaux, L., Birk, M., Wagner, G., Schreier, F., Xu, J., Vogt, P., Trautmann, T., and Yasui, M.: Validation of stratospheric and mesospheric ozone observed by SMILES from International Space Station, *Atmos. Meas. Tech.*, 6, 2311-2338, doi:10.5194/amt-6-2311-2013, 2013.
- Kramarova, N. A., Frith, S. M., Bhartia, P. K., McPeters, R. D., Taylor, S. L., Fisher, B. L., Labow, G. J., and DeLand, M. T.: Validation of ozone monthly zonal mean profiles obtained from the version 8.6 Solar Backscatter Ultraviolet algorithm, *Atmos. Chem. Phys.*, 13, 6887–6905, doi:10.5194/acp-13-6887-2013, 2013.
- Kramarova, N. A., Bhartia, P. K., Jaross, G., Moy, L., Xu, P., Chen, Z., DeLand, M., Froidevaux, L., Livesey, N., Degenstein, D., Bourassa, A., Walker, K. A., and Sheese, P.: Validation of ozone profile retrievals derived from the OMPS LP version 2.5 algorithm against correlative satellite measurements, *Atmos. Meas. Tech.*, 11, 2837-2861, doi:10.5194/amt-11-2837-2018, 2018.
- [Labow, G. J., Ziemke, J. R., McPeters, R. D., Haffner, D. P., and Bhartia, P. K.: A total ozone-dependent ozone profile climatology based on ozonesondes and Aura MLS data, *J. Geophys. Res. Atmos.*, 120, 2537–2545. doi: 10.1002/2014JD022634, 2015.](#)
- Livesey, N. J., Read, W. G., Froidevaux, L., Waters, J. W., Santee, M. L., Pumphrey, H. C., Wu, D. L., Shippony, Z., and Jarnot, R. F.: The UARS Microwave Limb Sounder version 5 data set: Theory, characterization, and validation, *J. Geophys. Res.*, 108, 4378, doi:10.1029/2002JD002273, D13, 2003.
- [McPeters, R. D., and Labow, G. J.: Climatology 2011: An MLS and sonde derived ozone climatology for satellite retrieval algorithms, *J. Geophys. Res.*, 117, D10303, doi:10.1029/2011JD017006, 2012.](#)
- McPeters, R. D., Bhartia, P. K., Haffner, D., Labow, G. J. and Flynn, L.: The version 8.6 SBUV ozone data record: An overview, *J. Geophys. Res. Atmos.*, 118, 8032–8039, doi:10.1002/jgrd.50597, 2013.
- McPeters, R., Frith, S., Kramarova, N., Ziemke, J., and Labow, G.: Trend quality ozone from NPP OMPS: the version 2 processing, *Atmos. Meas. Tech.*, 12, 977-985, doi:10.5194/amt-12-977-2019, 2019.
- Molina, M. J., and Rowland, F. S.: Stratospheric sink for chlorofluoromethanes: Chlorine atomic catalysed destruction of ozone, *Nature*, 249, 810–812, doi:10.1038/249810a0, 1974.

- Molod, A., Takacs, L., Suarez, M., and Bacmeister, J.: Development of the GEOS-5 atmospheric general circulation model: evolution from MERRA to MERRA2, *Geosci. Model Dev.*, 8, 1339–1356, doi:10.5194/gmd-8-1339-2015, 2015.
- Nielsen, J. E., Pawson, S., Molod, A., Auer, B., da Silva, A. M., Douglass, A. R., Duncan, B., Liang, Q., Manyin, M., Oman, L. D., Putman, W., Strahan, S. E., and Wargan, K.: Chemical mechanisms and their applications in the Goddard Earth Observing System (GEOS) earth system model, *J. Adv. Model. Earth Sy.*, 9, 3019–3044, doi:10.1002/2017MS001011, 2017.
- Ogawa, H., Kawabata, K., Yonekura, Y., and Iwasaka, Y.: Diurnal and Seasonal Variations of Strato-Mesospheric Ozone, *J. Geomag. Geoelectr.*, 49, 1115–1126, 1996.
- Orbe, C., Oman, L. D., Strahan, S. E., Waugh, D. W., Pawson, S., Takacs, L. L., and Molod, A. M.: Large-scale atmospheric transport in GEOS replay simulations, *Journal of Advances in Modeling Earth Systems*, 9, 2545–2560, doi:10.1002/2017MS001053, 2017.
- Parrish, A., Boyd, I. S., Nedoluha, G. E., Bhartia, P. K., Frith, S. M., Kramarova, N. A., Connor, B. J., Bodeker, G. E., Froidevaux, L., Shiotani, M., and Sakazaki, T.: Diurnal variations of stratospheric ozone measured by ground-based microwave remote sensing at the Mauna Loa NDACC site: measurement validation and GEOSCCM model comparison, *Atmos. Chem. Phys.*, 14, 7255–7272, doi:10.5194/acp-14-7255-2014, 2014.
- Pallister, R. C., and Tuck, A. F.: The diurnal variation of ozone in the upper stratosphere as a test of photochemical theory, *Q. J. R. Meteorol. Soc.*, 109, 271–284, 1983.
- Palm, M., Hoffmann, C. G., Golchert, S. H. W., and Notholt, J.: The ground-based MW radiometer OZORAM on Spitsbergen – description and status of stratospheric and mesospheric O₃-measurements, *Atmos. Meas. Tech.*, 3, 1533–1545, doi:10.5194/amt-3-1533-2010, 2010.
- Prather, M. J.: Ozone in the upper stratosphere and mesosphere, *J. Geophys. Res.*, 86, 5325–5338, 1981.
- Ricaud, P., Brillet, J., deLa Noë, J., Parisot, J. –P.: Diurnal and seasonal variations of stratomesospheric ozone: Analysis of ground-based microwave measurements in Bordeaux, France, *J. Geophys. Res.*, 96, 18,617–18,629, 1991.
- Sakazaki, T., Shiotani, M., Suzuki, M., Kinnison, D., Zawodny, J. M., McHugh, M., and Walker, K. A.: Sunset–sunrise difference in solar occultation ozone measurements (SAGE II, HALOE, and ACE–FTS) and its relationship to tidal vertical winds, *Atmos. Chem. Phys.*, 15, 829–843, doi:10.5194/acp-15-829-2015, 2015.

- Sakazaki, T., Fujiwara, M., Mitsuda, C., Imai, K., Manago, N., Naito, Y., Nakamura, T., Akiyoshi, H., Kinnison, D., Sano, T., Suzuki, M., and Shiotani, M.: Diurnal ozone variations in the stratosphere revealed in observations from the Superconducting Submillimeter-Wave Limb-Emission Sounder (SMILES) onboard the International Space Station (ISS), *J. Geophys. Res.-Atmos.*, 118, 2991–3006, doi:10.1002/jgrd.50220, 2013.
- Schanz, A., Hocke, K., and Kämpfer, N.: Daily ozone cycle in the stratosphere: global, regional and seasonal behaviour modeled with the Whole Atmosphere Community Climate Model, *Atmos. Chem. Phys.*, 14, 7645–7663, doi:10.5194/acp-14-7645-2014, 2014a.
- Schanz, A., Hocke, K., Kämpfer, N., Chabrilat, S., Inness, A., Palm, M., Notholt, J., Boyd, I., Parrish, A., and Kasai, Y.: The diurnal variation in stratospheric ozone from the MACC reanalysis, the ERA-Interim reanalysis, WACCM and Earth observation data: characteristics and intercomparison, *Atmos. Chem. Phys. Discuss.*, 14, 32667–32708, doi:10.5194/acpd-14-32667-2014, 2014b.
- Schranz, F., Fernandez, S., Kämpfer, N., and Palm, M.: Diurnal variation in middle-atmospheric ozone observed by ground-based microwave radiometry at Ny-Ålesund over 1 year, *Atmos. Chem. Phys.*, 18, 4113–4130, doi:10.5194/acp-18-4113-2018, 2018.
- Strahan, S. E., Duncan, B. N., and Hoor, P.: Observationally de-rived transport diagnostics for the lowermost stratosphere and their application to the GMI chemistry and transport model, *Atmos. Chem. Phys.*, 7, 2435–2445, doi:10.5194/acp-7-2435-2007, 2007.
- Stolarski, R. S. and Cicerone, R. J.: Stratospheric chlorine: A possible sink for ozone, *Canadian Journal of Chemistry*, 52(8): 1610-1615, doi:10.1139/v74-233, 1974.
- Studer, S., Hocke, K., Schanz, A., Schmidt, H., and Kämpfer, N.: A climatology of the diurnal variations in stratospheric and mesospheric ozone over Bern, Switzerland, *Atmos. Chem. Phys.*, 14, 5905–5919, doi:10.5194/acp-14-5905-2014, 2014.

Table 1. Ozone Observations and Corresponding Measurement Times.

Instrument	Measurement Time at Equator	Period of Data (years)	Reference
Aura MLS (v4.2)	1:30pm; 1:30am	2004-2018	Froidevaux, et al. , 2008
SAGE III/ISS (aO3)	Local sunrise; Local sunset	2017-2018	Chu and Veiga, 1998
OMPS LP (v2.5) OMPS NP (v2.6)	1:30pm	2012-2018	LP: Kramarova et al., 2018 NP: McPeters et al., 2019
SBUV/2 (v8.6) ascending profiles NOAA-16, NOAA-18, NOAA-19	Orbit drifts slowly between 2pm and 4pm	NOAA-16: 2000-2007 NOAA-18: 2005-2012 NOAA-19: 2009-2018	McPeters et al., 2013 Bhartia et al., 2013
SBUV/2 (v8.6) descending profiles NOAA-16, NOAA-17	Orbit drifts slowly between 8am and 10am	NOAA-16: 2012-2014 NOAA-17: 2005-2011	McPeters et al., 2013 Bhartia et al., 2013
UARS MLS (v5)	Complete cycle 36 days	1991-1999	LivesayLivesey et al., 2003
SMILES (v2.4)	Complete cycle 30 days	Oct 2009-Apr 2010	Kasai et al., 2013



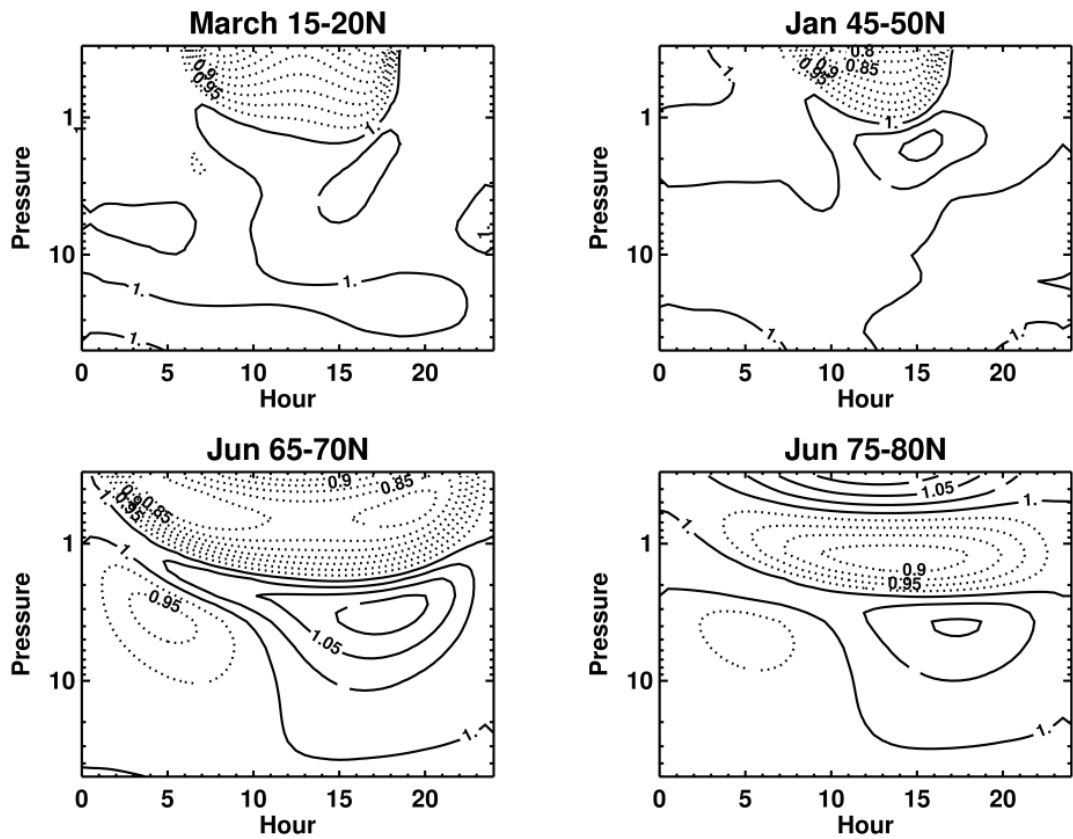
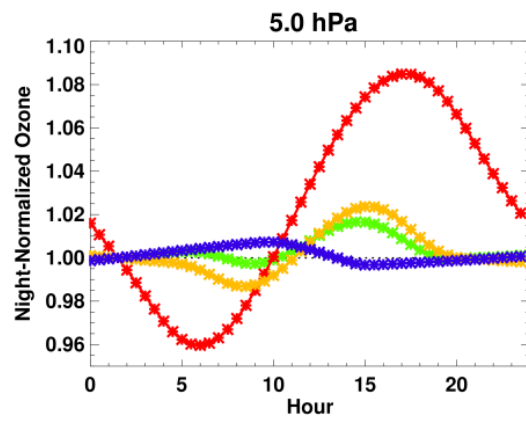
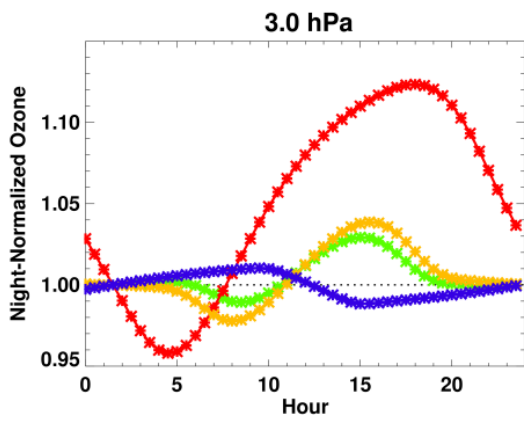
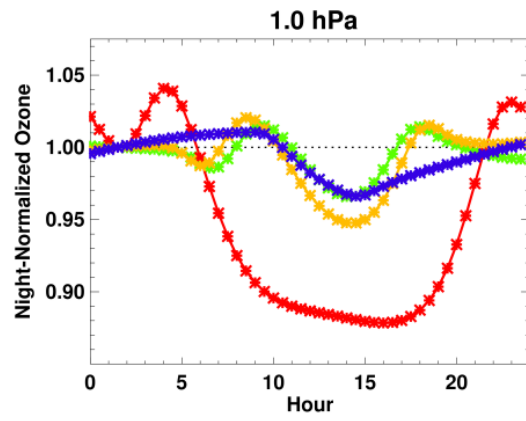
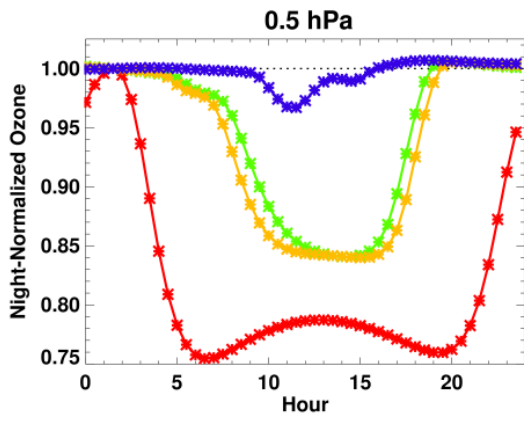


Figure 1. Contour plot of the GEOS-GMI diurnal ozone climatology (GDOC) normalized to the midnight value as a function of hour and pressure for March at 15-20° N (top left); January at 45-50° N (top right); June at 65-70° N (bottom left); and June at 75-80° N (bottom right). The contour interval is 0.025 (2.5%). The climatology is shown at levels from 3050 hPa to 0.3 hPa.



—* Mar
 —* Jun
 —* Sep
 —* Dec

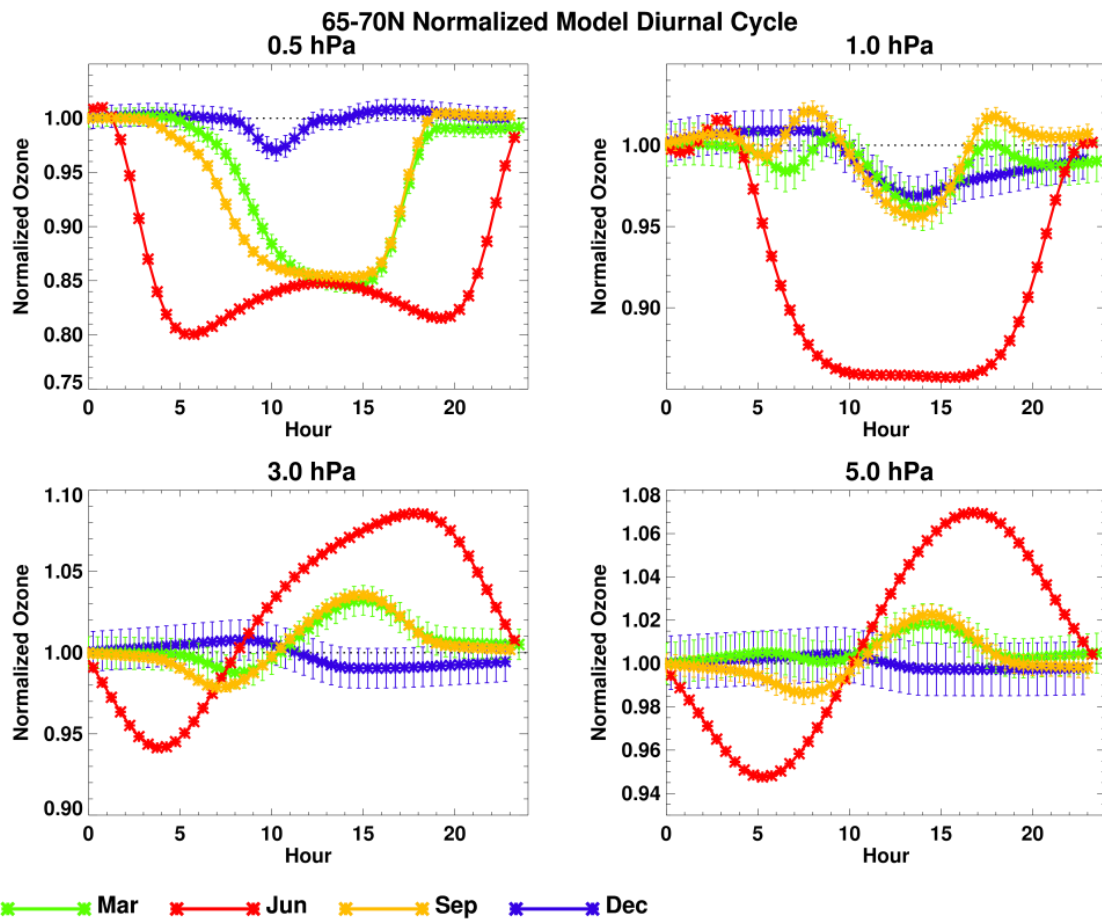


Figure 2. GDOC at 65-70° N as a function of season on four pressure levels: 0.5 hPa (top left); 1 hPa (top right); 3 hPa (bottom left); and 5 hPa (bottom right). Seasons are represented by monthly output in March, June, September and December. The diurnal signal is plotted as a function of hour (30-minute resolution) and is normalized to the 1:30am value. The error bars are 2*standard error of the mean, as described in the text. The model uncertainty is largest in winter, when the day to day and longitudinal variability of model ozone is greatest.

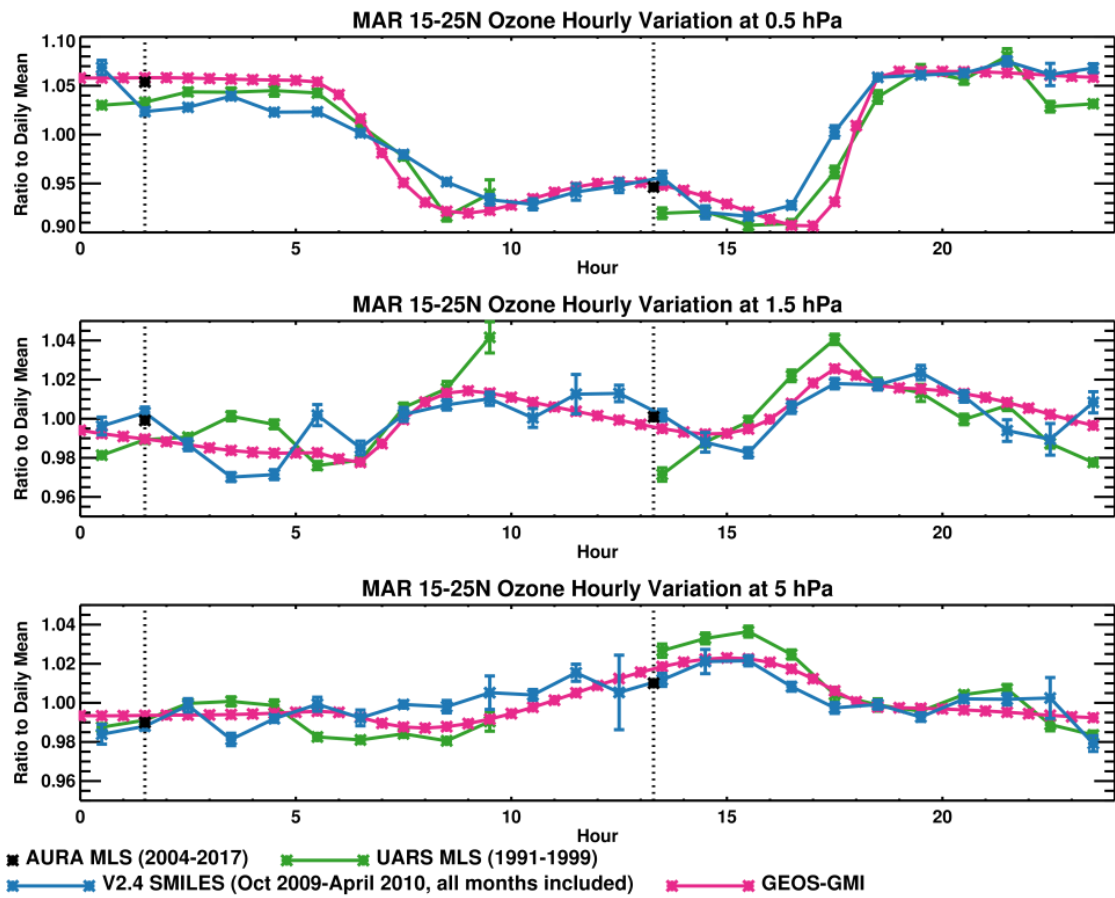


Figure 3.

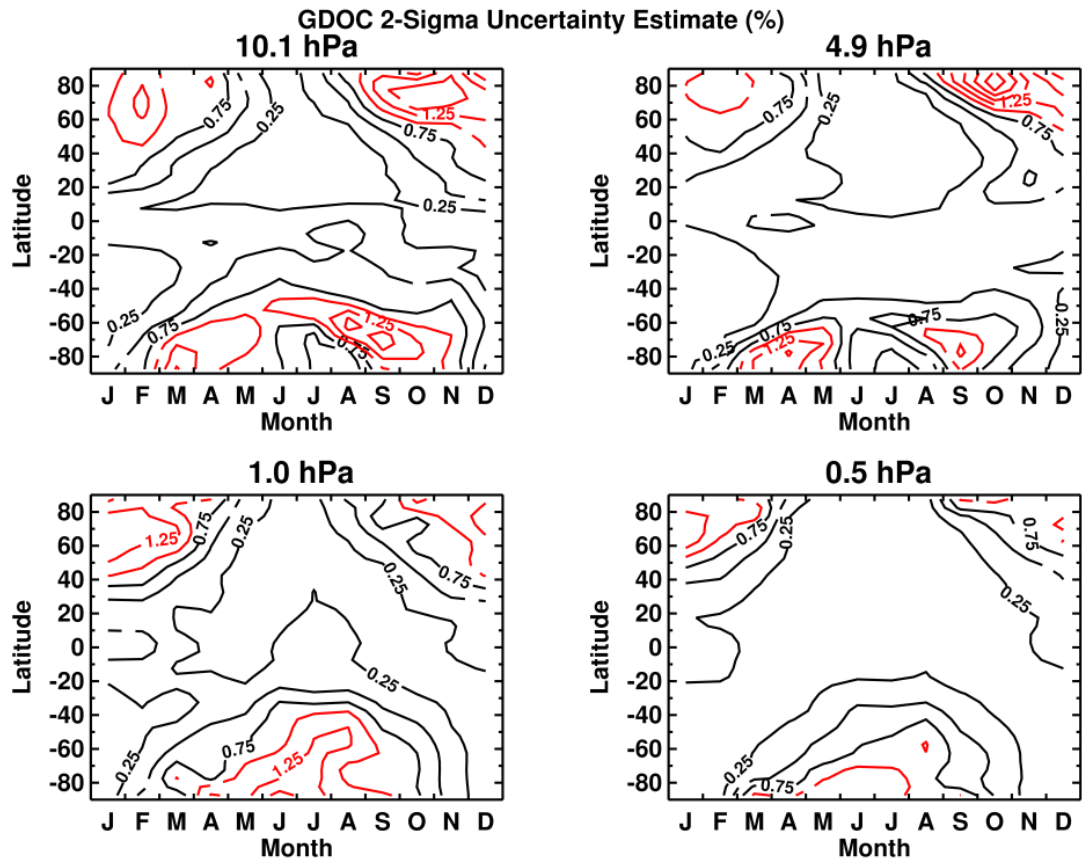


Figure 3. GDOC uncertainty estimates at noon local solar time, plotted as a function of month and latitude on four pressure levels: 10.1 hPa (top left); 4.9 hPa (top right); 1.0 hPa (bottom left); and 0.5 hPa (bottom right). The uncertainty is defined as the standard error of the mean in each bin, computed assuming 720 independent data points per bin. Contours of 1% and greater are highlighted in red.

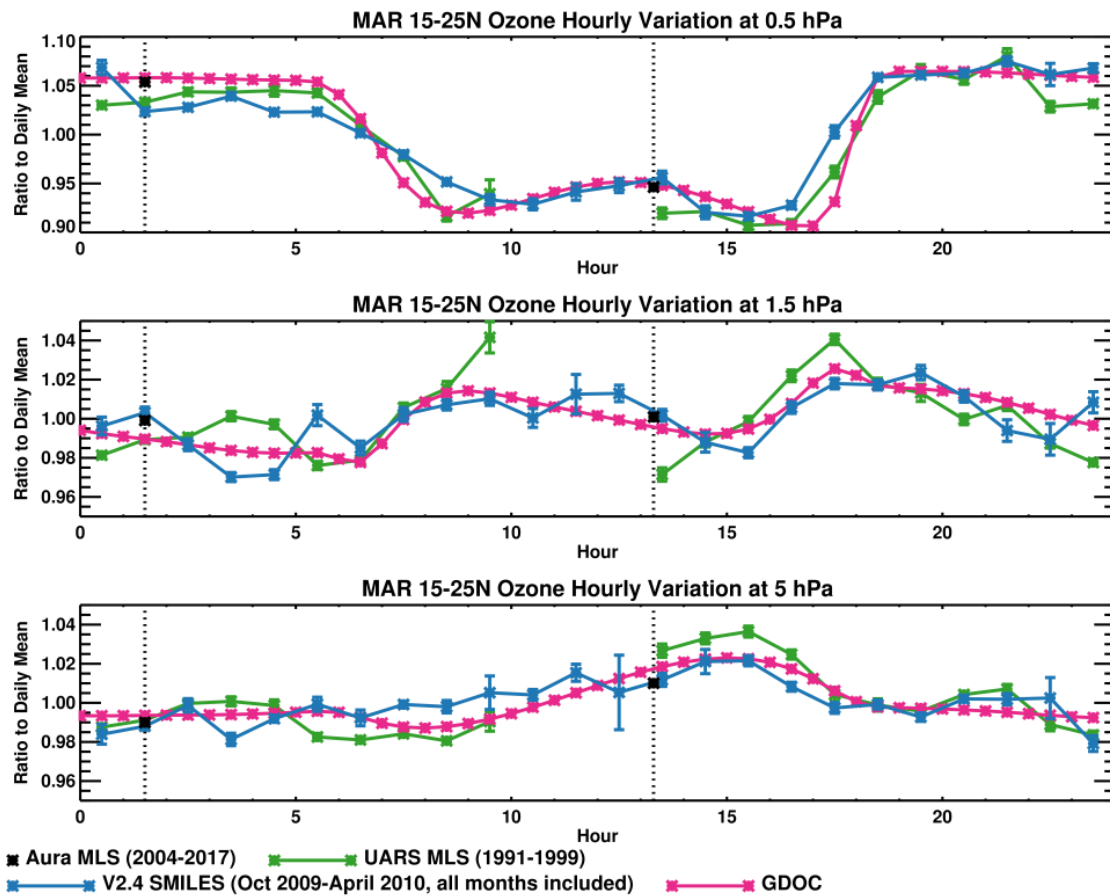
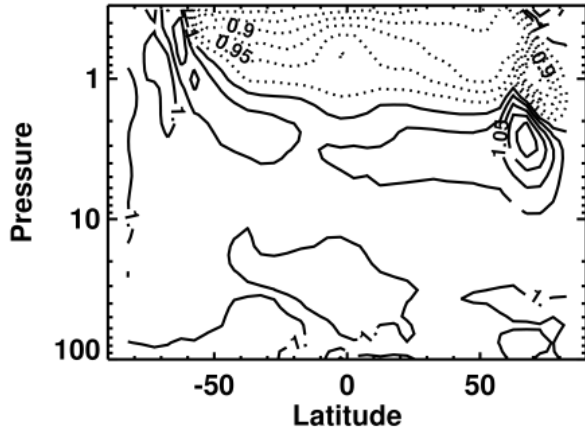
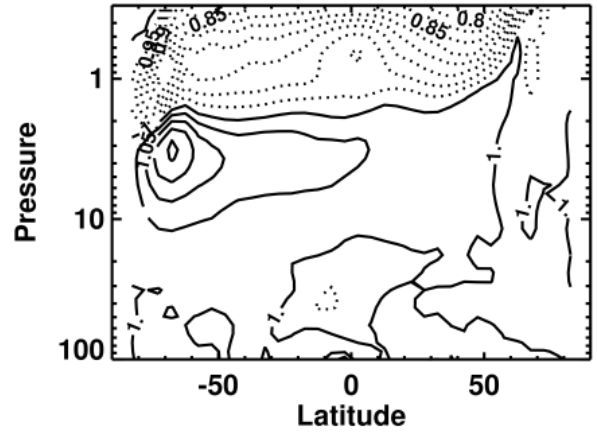


Figure 4. Diurnal variations as derived from SMILES (blue), UARS MLS (green) and Aura MLS (black symbols), compared to GDOC (red), plotted as a function of hour at three pressure levels: 0.5 hPa (top), 1.5 hPa (middle panel), and 5 hPa (bottom panel). Each product is normalized by its daily mean value, and the ratio is plotted. The black dotted lines indicate the two daily Aura MLS measurement times. UARS MLS means from 10am-1pm are not computed due to limited sampling. The error bars are 2* standard error of the mean. For the model and most satellite averages, this error is smaller than the symbol thickness.

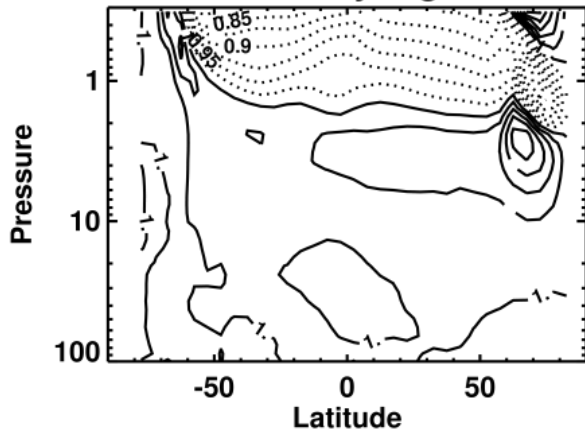
Jun AURA MLS Day/Night Ratio



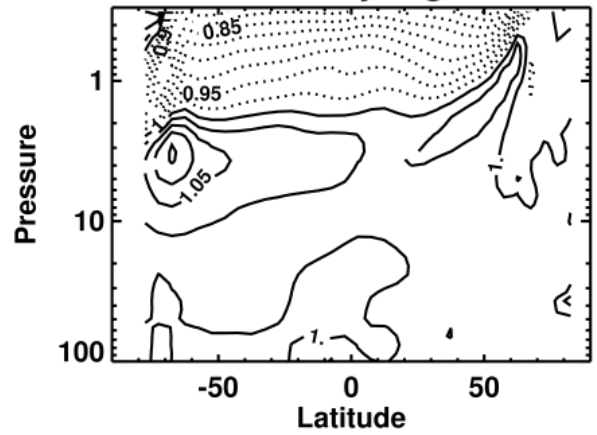
Dec AURA MLS Day/Night Ratio



Jun Model Day/Night Ratio



Dec Model Day/Night Ratio



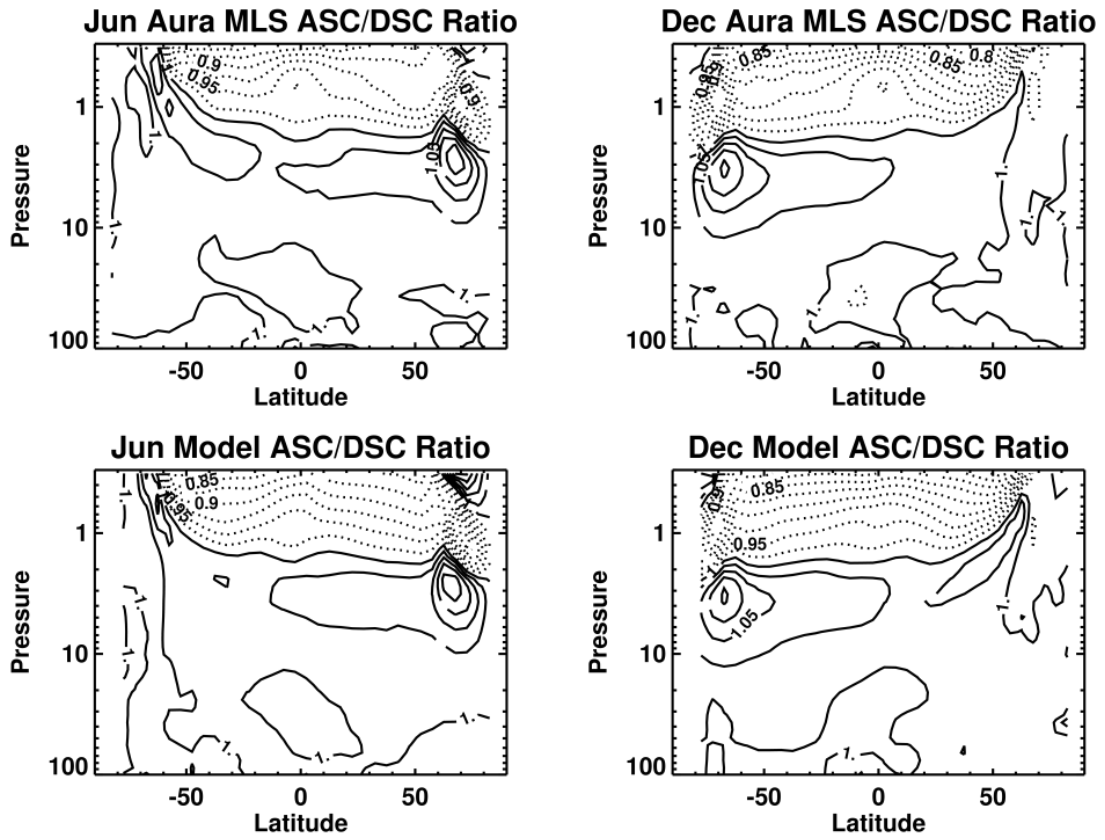
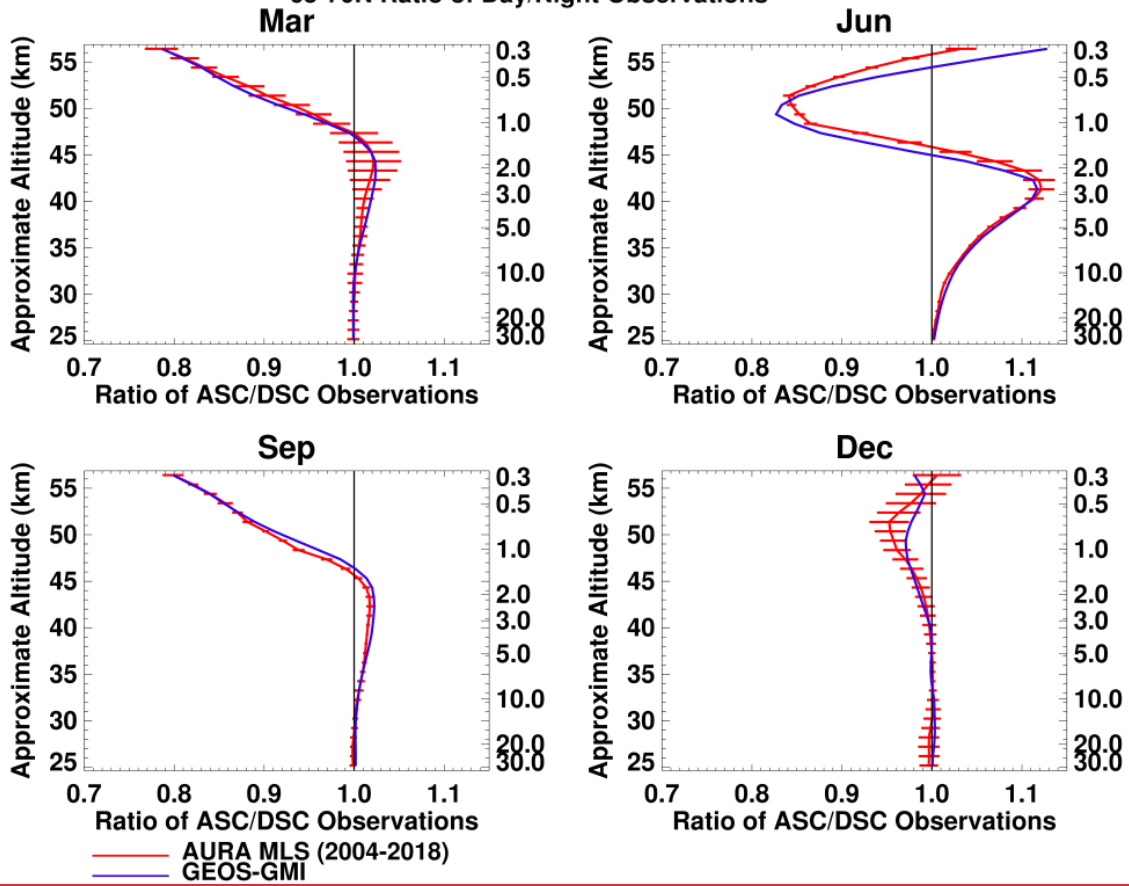
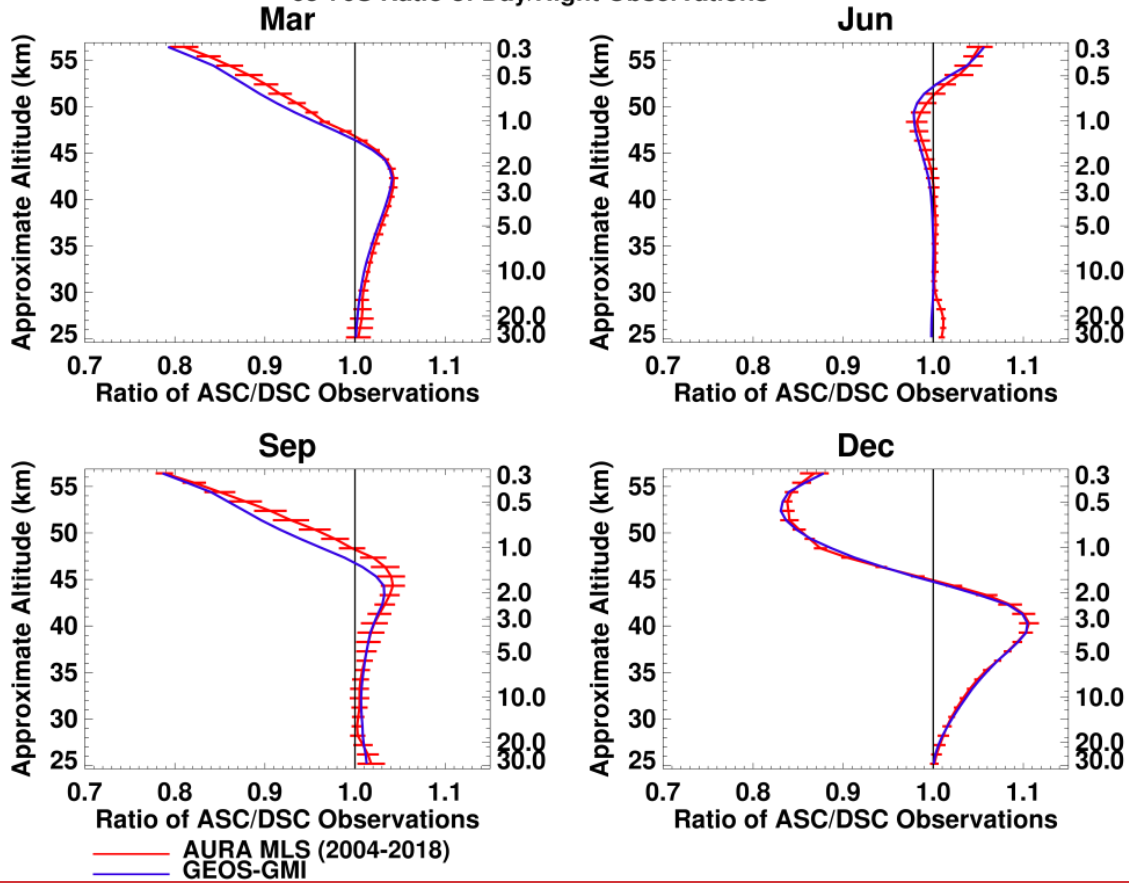


Figure 45. Aura MLS (top) and GDOC (bottom) average ratio of ascending (day at most latitudes) to descending (night at most latitudes) average ozone in June (left) and December (right) as a function of latitude and pressure from 100 hPa to 0.3 hPa. Contour interval is 0.025 (2.5%). GDOC is sampled at Aura MLS measurement times.

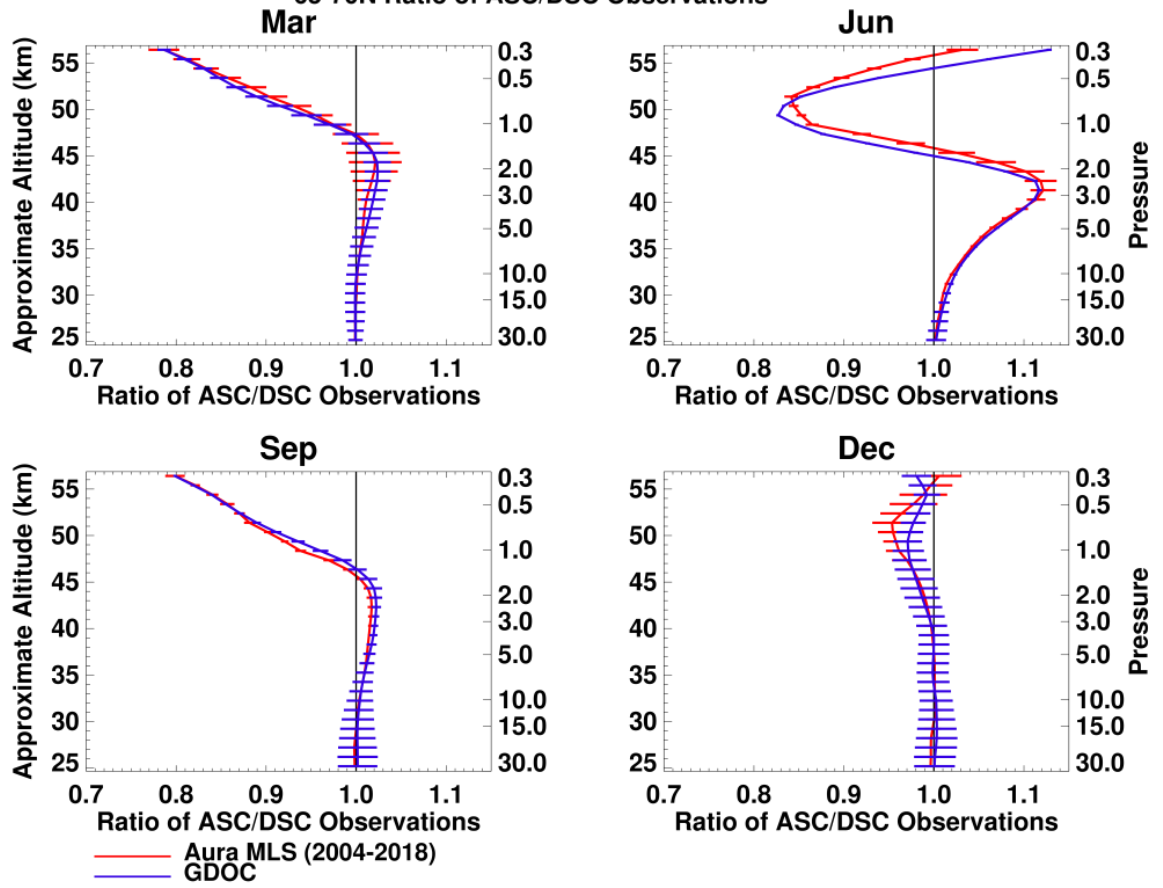
65-70N Ratio of Day/Night Observations



65-70S Ratio of Day/Night Observations



65-70N Ratio of ASC/DSC Observations



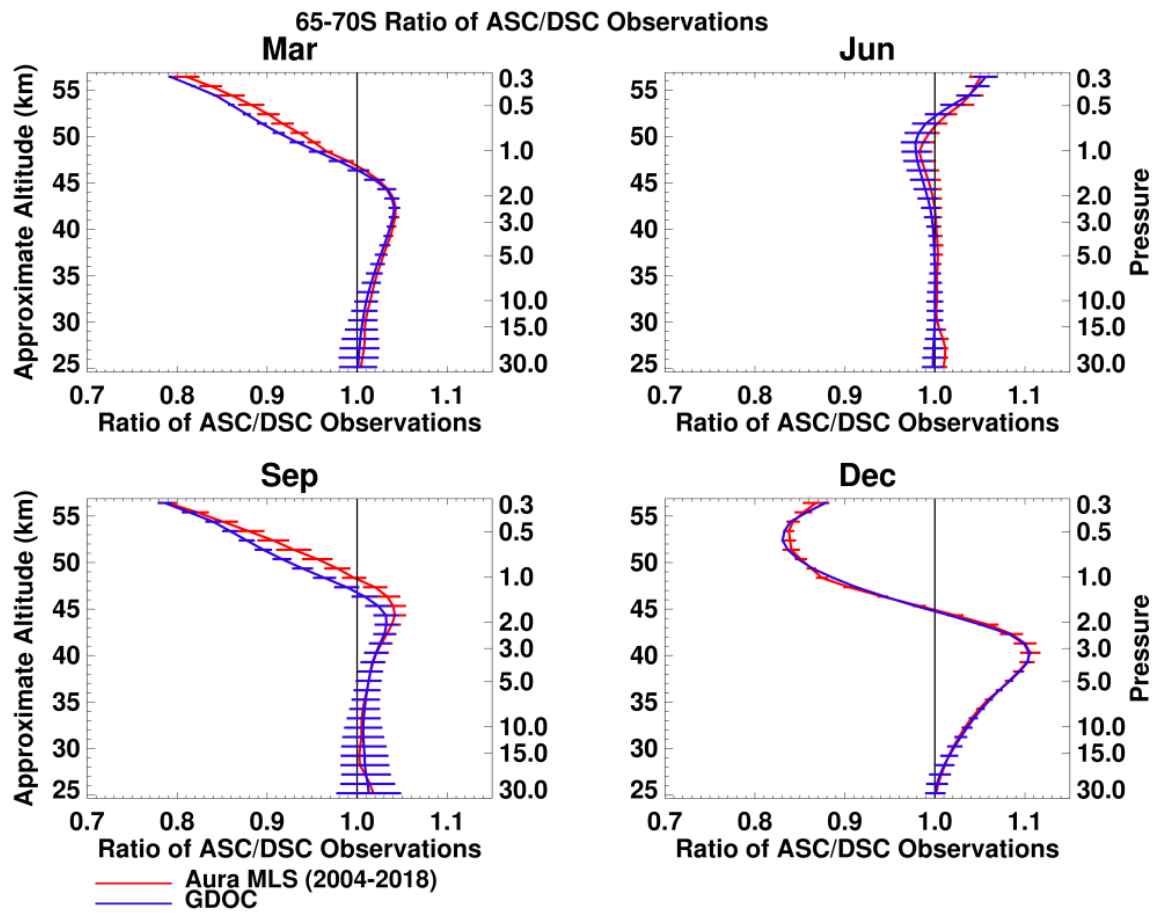
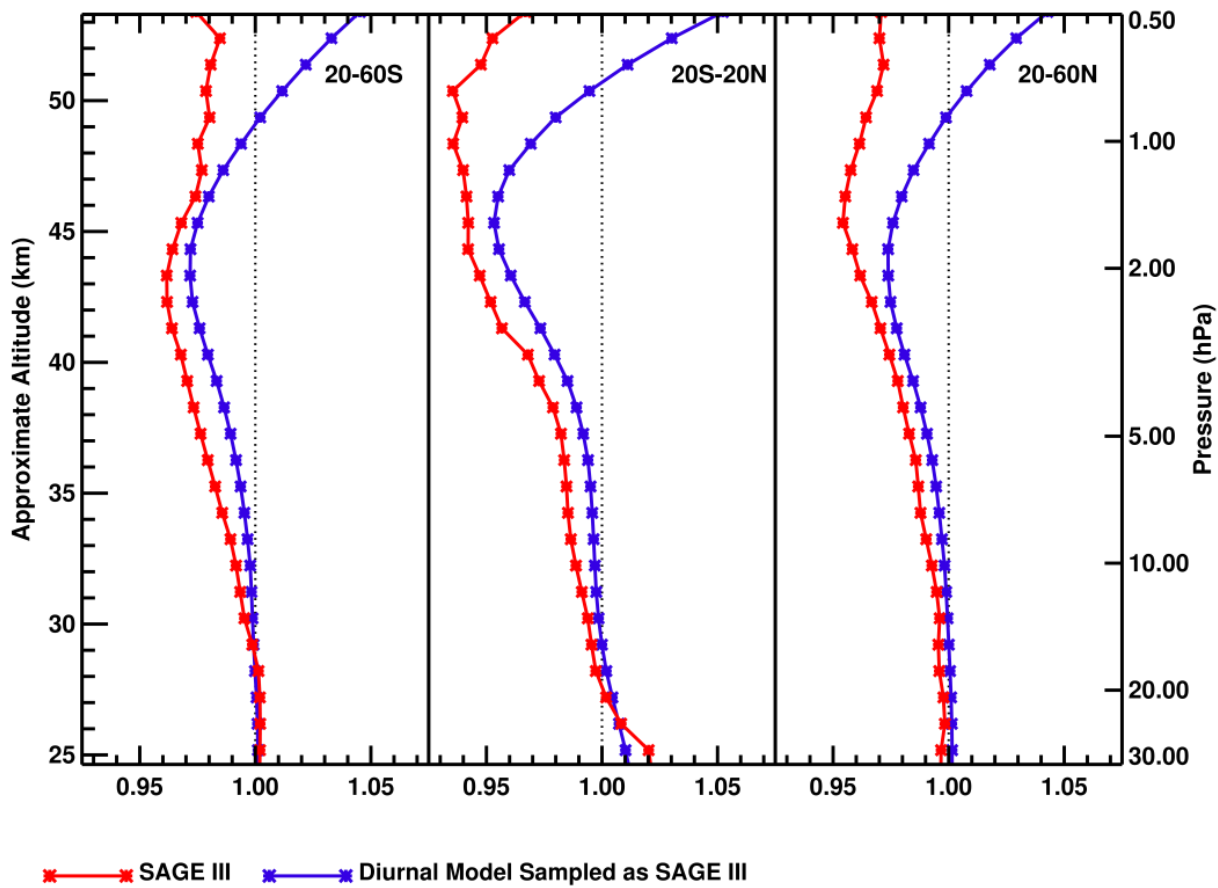


Figure 56. Profile of mean ratio of ascending (day at most latitudes) to descending (night at most latitudes) measurements at 65-70° N (top four panels) and 65-70° S (bottom four panels) from Aura MLS (2004-2018) and GDOC sub-sampled at Aura MLS profile locations/times. Four panels show results for March, June, September and December. Error bars indicate the two-sigma standard deviation of Aura MLS day-night ascending/descending ratio profiles from year to year. We show the standard deviation to highlight the interannual variability of the ratio observed by Aura MLS. The model error bars are 2* standard error of the mean, as described in the text.

ISS SAGE III SR/SS



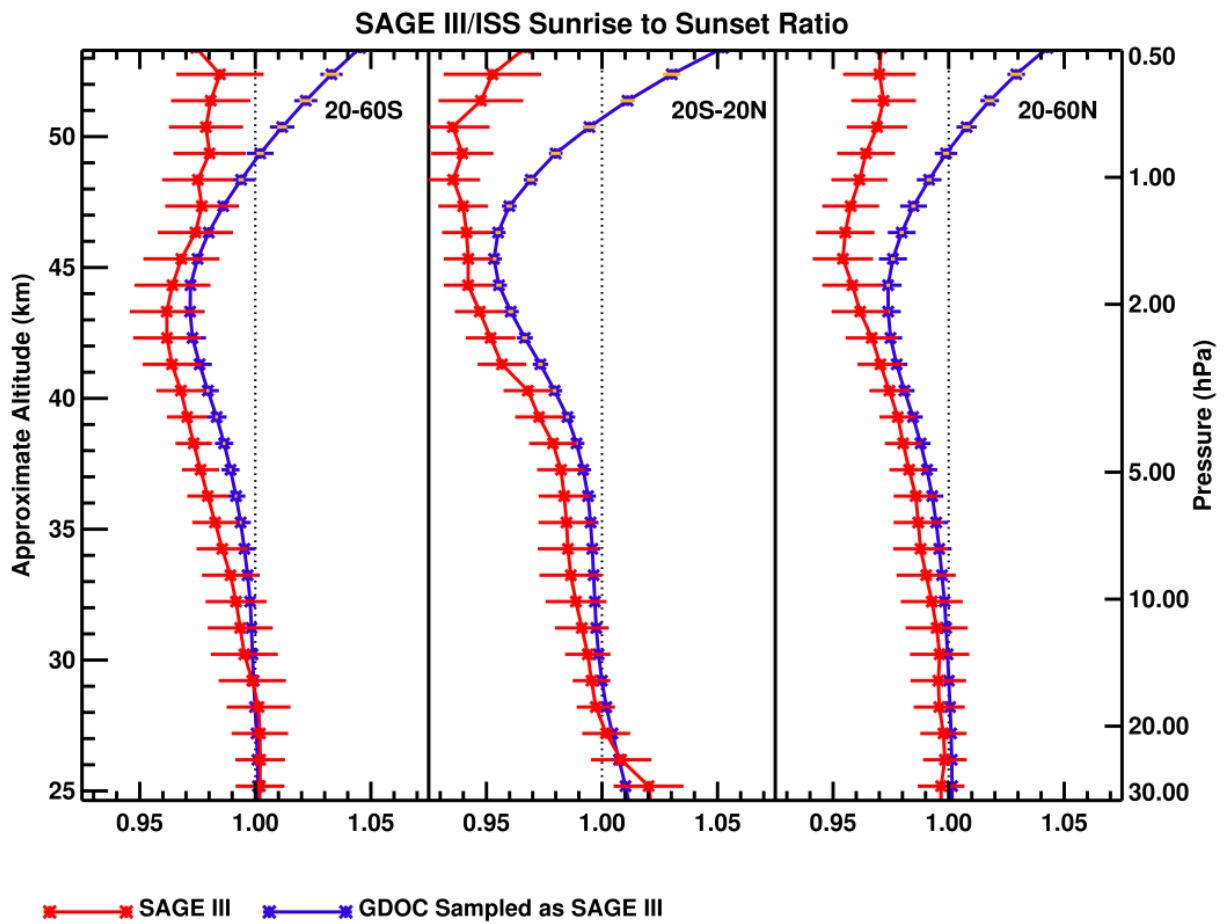
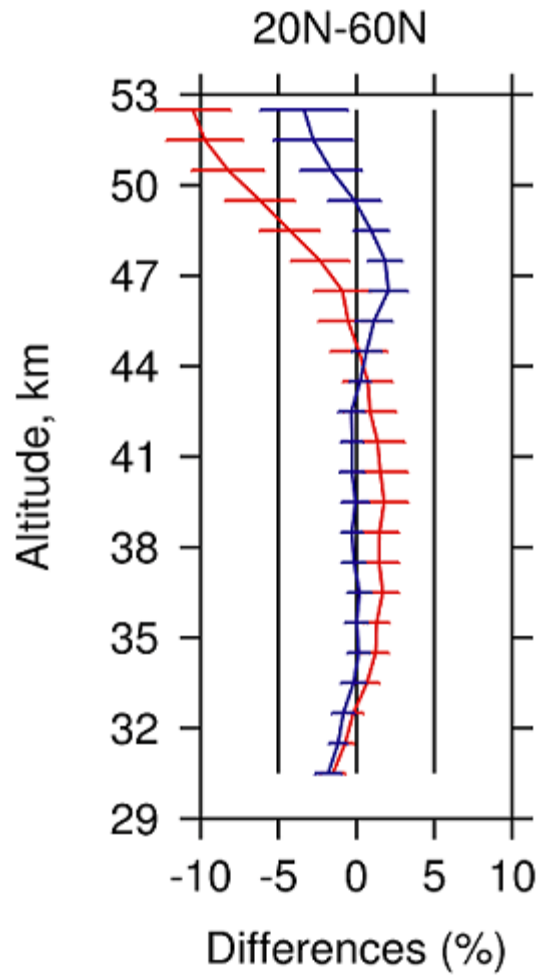
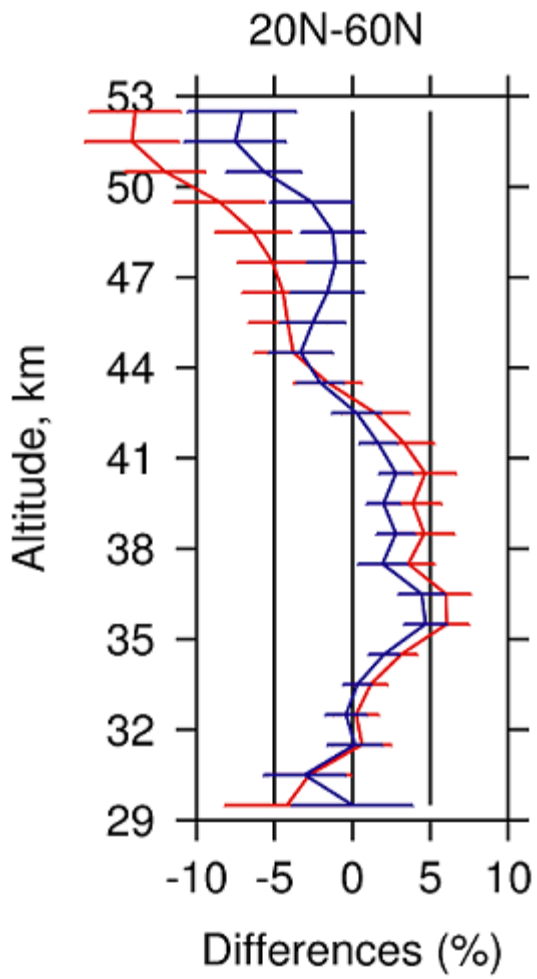


Figure 67. Ratio of mean sunrise to mean sunset ozone values from the SAGE III/ISS (red) and from GDOC (blue) sampled at SAGE III/ISS profile locations/times from 2017-2018. Ratios are shown averaged in broad latitude bands: 20-60° S (left); 20° S to 20° N (middle); and 20-60° N (right). The SAGE error bars denote 2*standard error of the mean (sem), computed as the root mean square of the sunrise and sunset sem values. Note that SAGE III measurements are such that the spatial and time sampling are different for the sunrise and sunset mean profiles. The blue error bars for GDOC indicate the variability of the SAGE-sampled reconstructions (computed the same way as SAGE sem). The overlaid orange error bars (roughly the width of the plotting symbol) represents the model uncertainty, computed as the root mean square of the model standard deviation profiles at SAGE sampling, divided by the square root of n (=720).

SAGE III/ISS – OMPS LP

SAGE III/ISS-Aura MLS



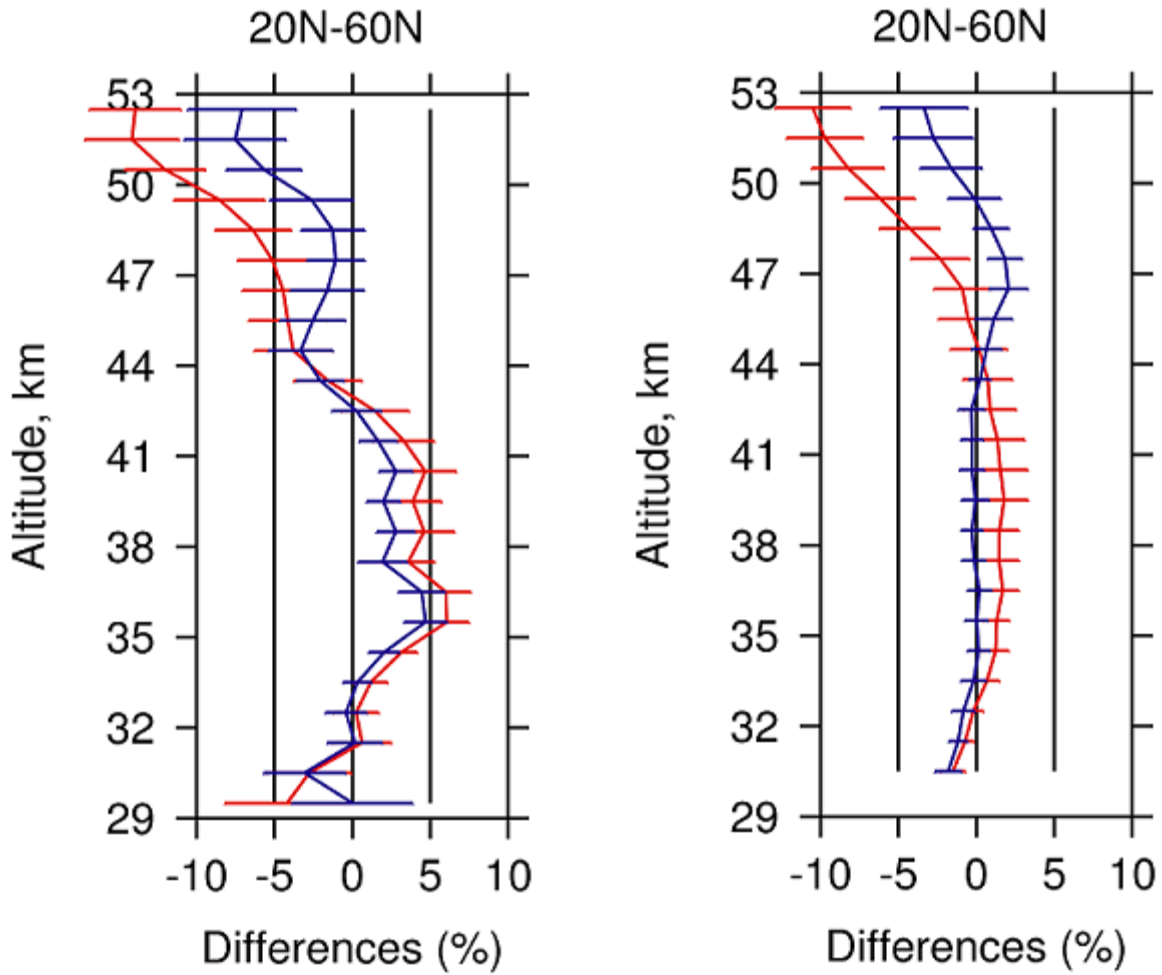
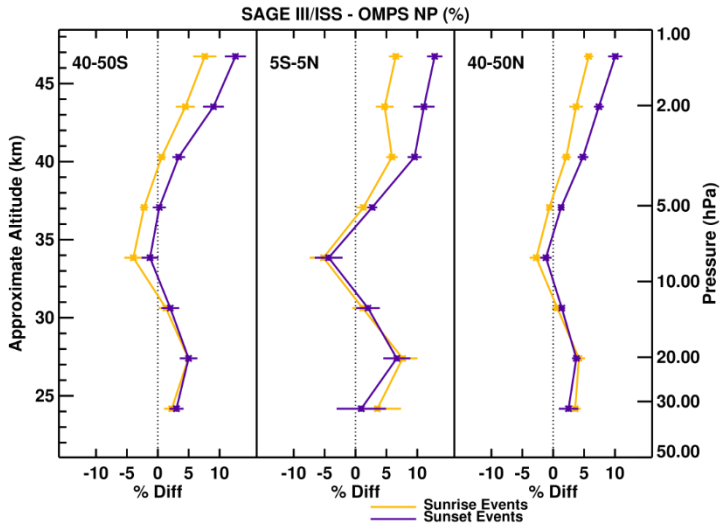
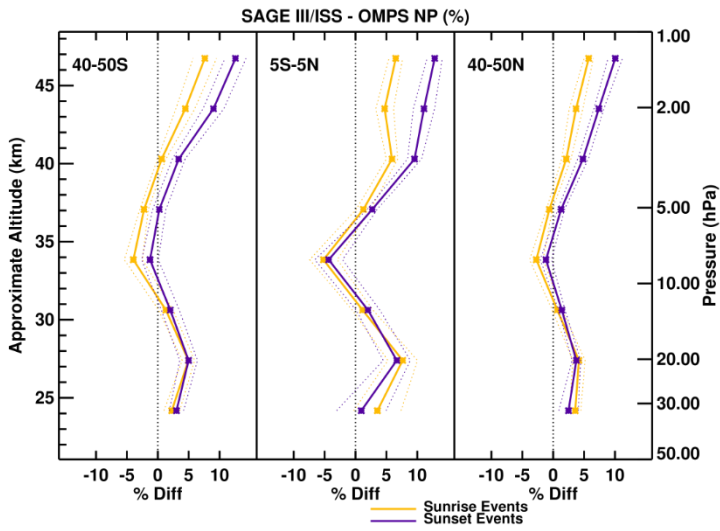


Figure 78. Profile of mean differences between SAGE III/ISS and OMPS Limb Profiler (left) and Aura MLS (right, daytime measurements only) averaged from 20° N to 60° N, expressed as percent difference as a function of altitude (km). Sunrise and sunset profiles are included in the mean difference. The red curve shows the original mean difference, while the blue curve shows the same comparison after using GDOC to adjust the SAGE profiles to an equivalent measurement time of 1:30pm to correspond to OMPS and Aura measurements. The error bars are the standard deviation (1-sigma; the standard error of the mean is smaller than the line width).



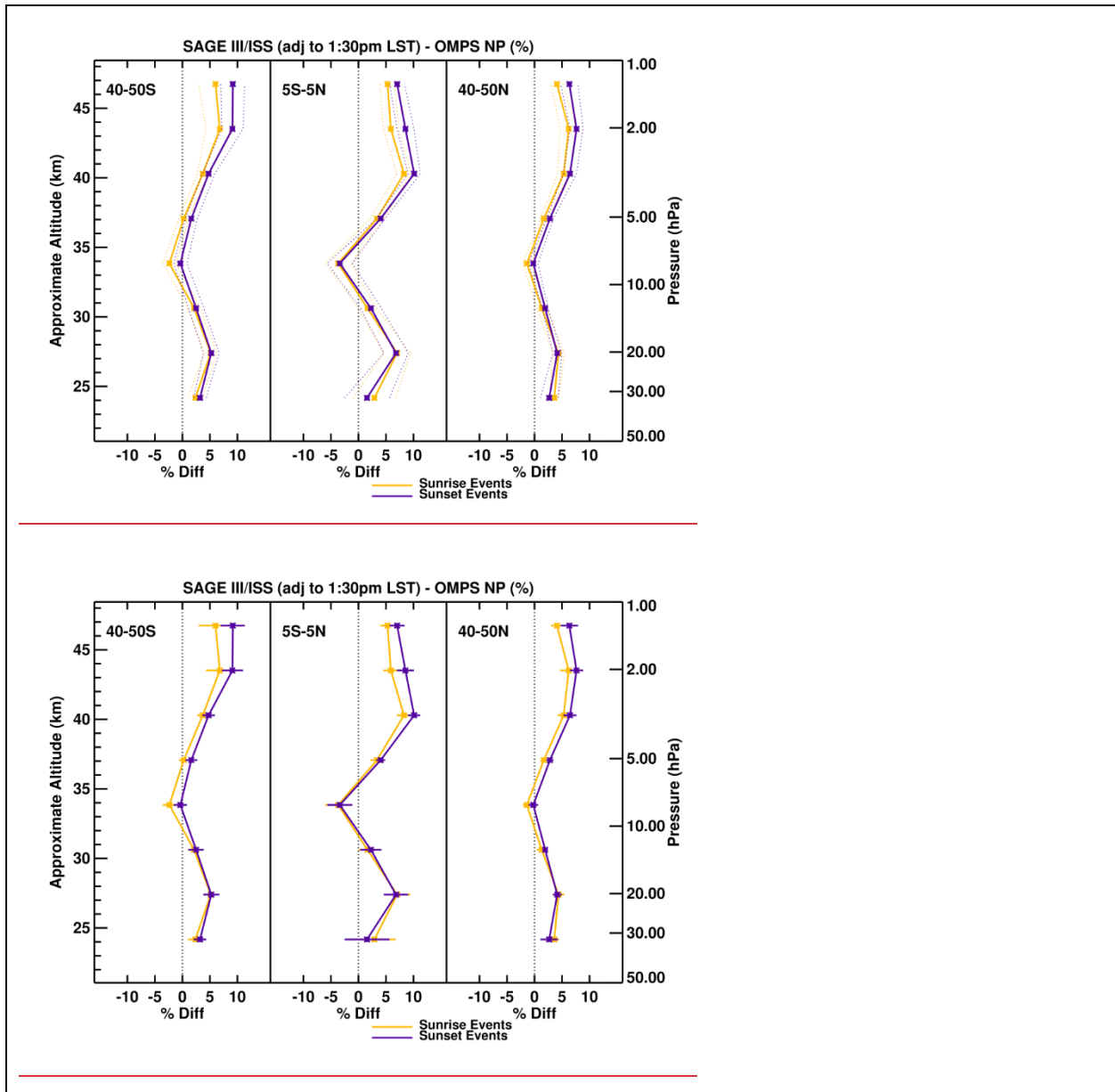
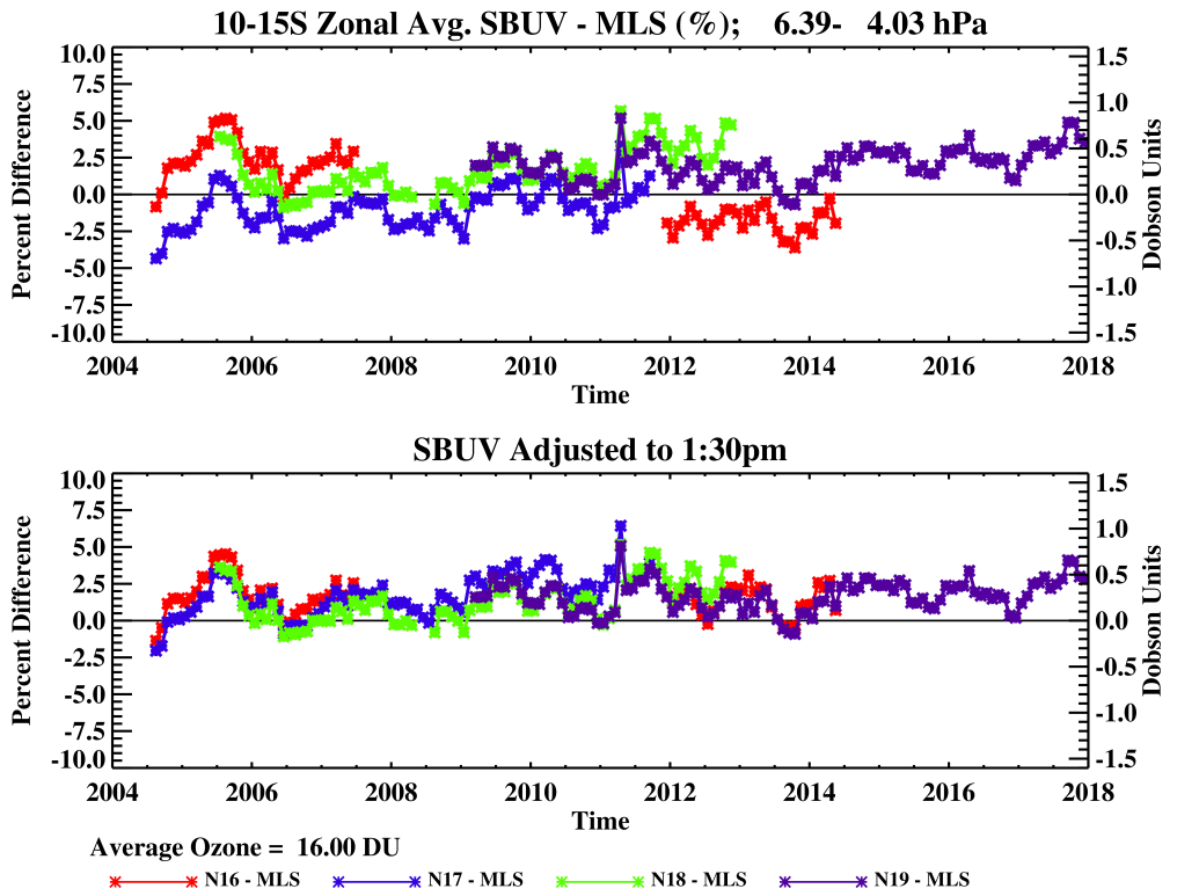


Figure 89. Profile of mean differences between SAGE III/ISS and OMPS Nadir Profiler (percent difference) as a function of pressure (hPa) separated by SAGE III/ISS sunrise and sunset profiles. Top panel shows original differences and bottom panel shows differences after the SAGE III/ISS profiles have been adjusted to the equivalent measurement time of the OMPS NP profiles. The error bars represent 2*standard error of the mean, based on the month to month variability only.



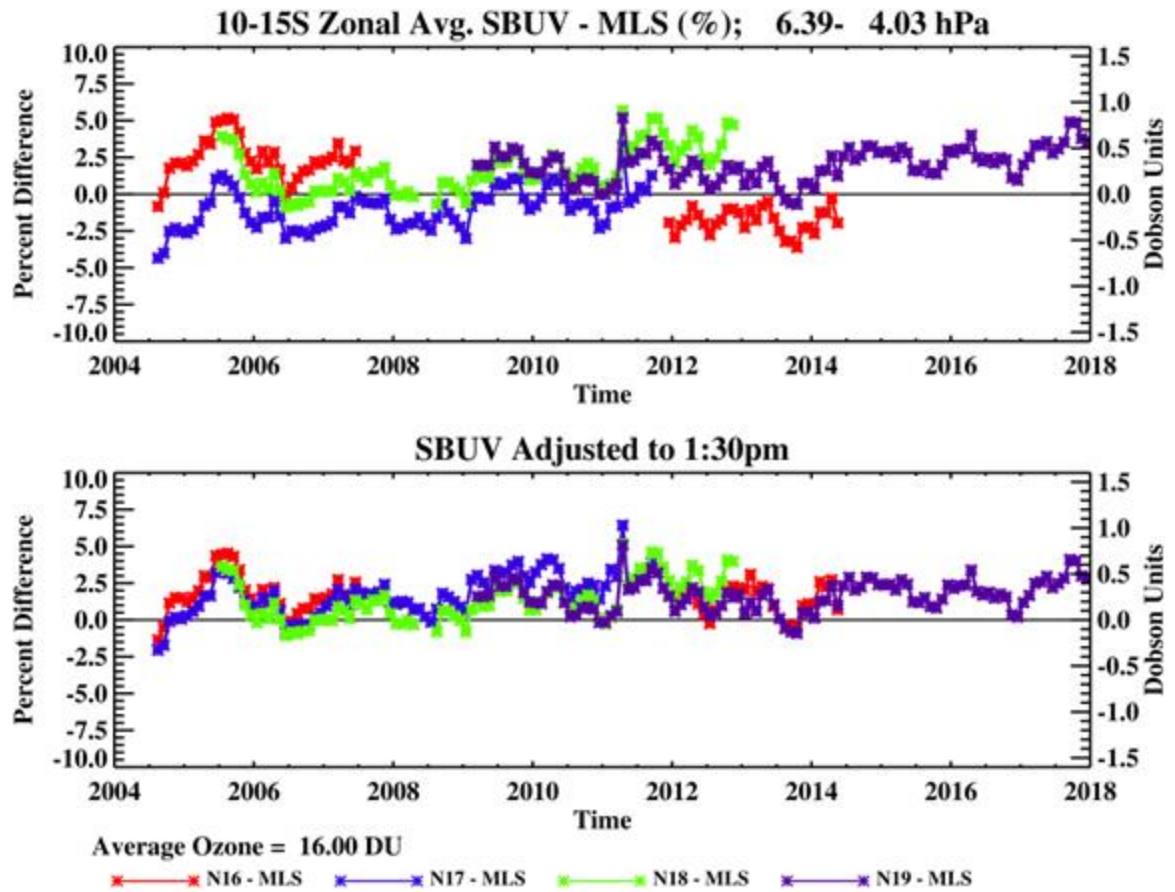


Figure 910. Time series of NOAA-16 through NOAA-19 SBUV zonal mean data relative to Aura MLS from 2004-2018 in the 10-15° S latitude band and 6-4 hPa pressure layer. Top panel shows original differences and bottom panel shows differences after individual SBUV instruments have been adjusted to a common time of 1:30pm, to coincide with the Aura MLS measurement time. Monthly zonal means of both SBUV and MLS are well sampled such that the uncertainty of 2 * standard error of the mean is smaller than the plot symbols.

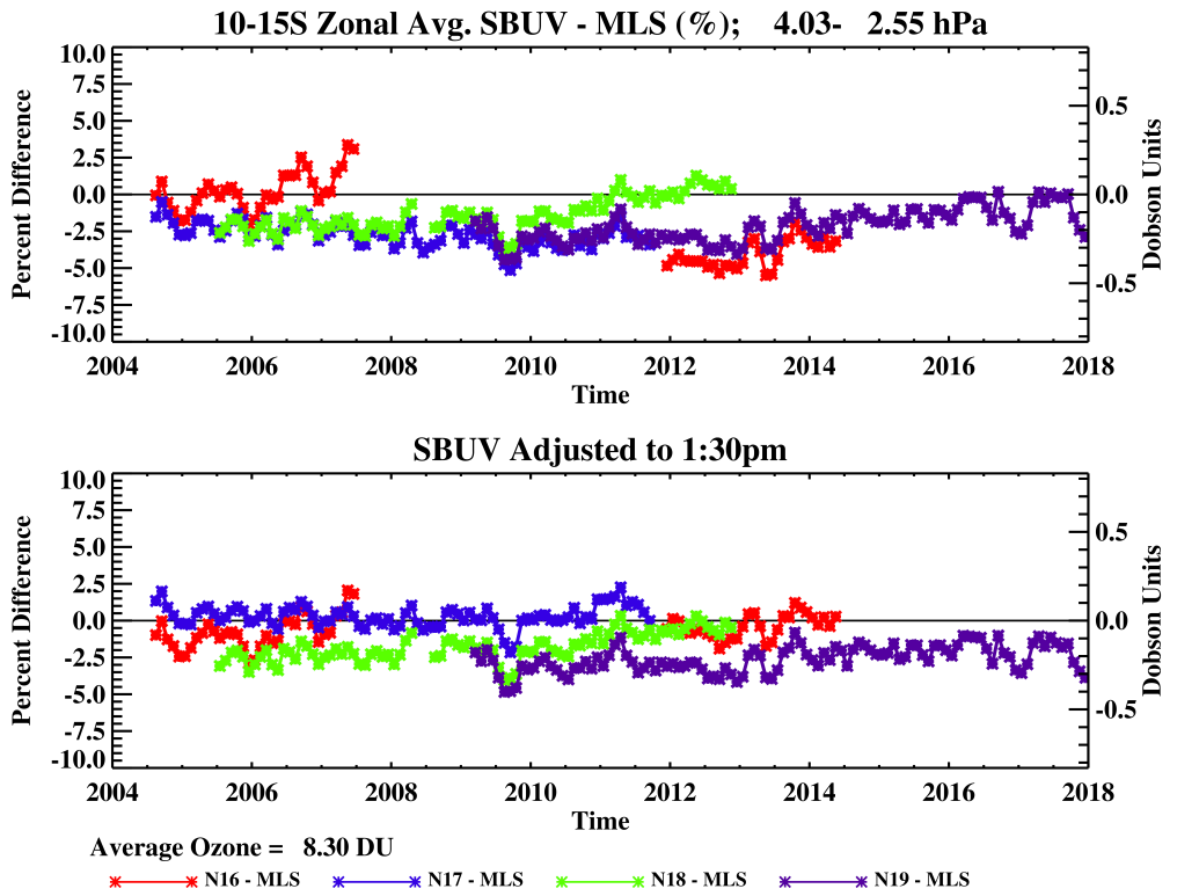


Figure 10.

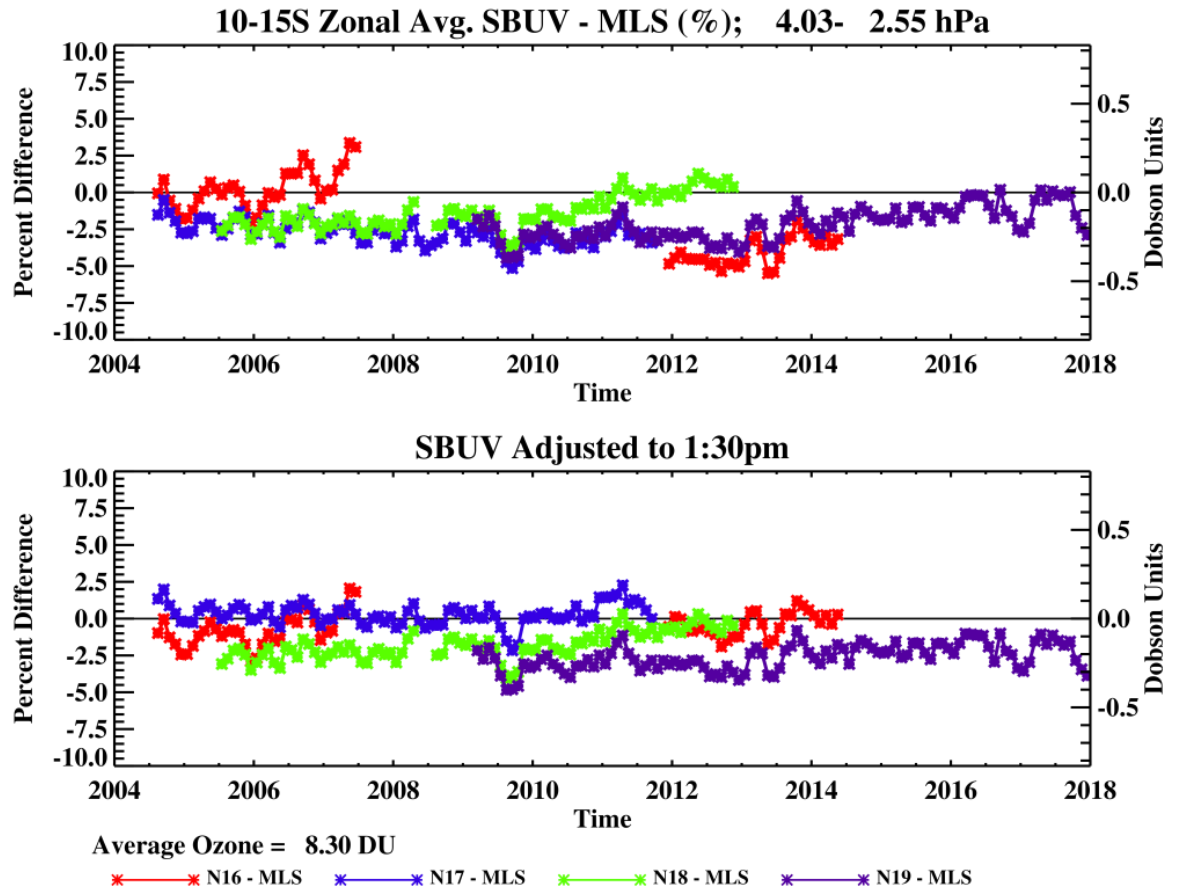
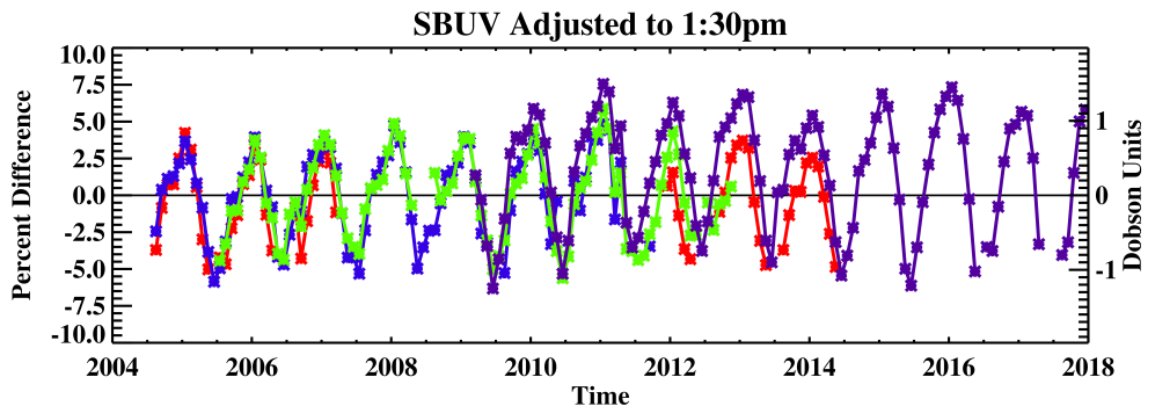
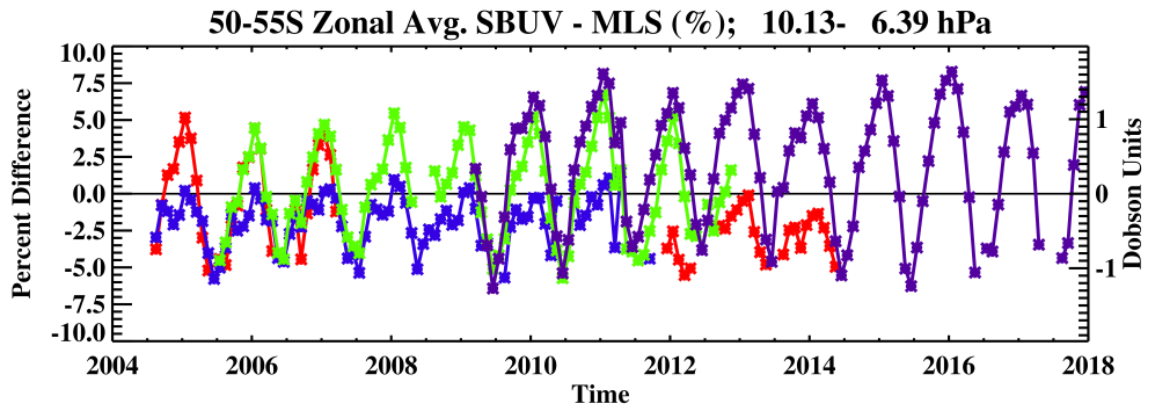


Figure 11. Same as Figure 10 but for 10-15° S latitude band at 4-2.5 hPa layer.



Average Ozone = 19.79 DU

* N16 - MLS
 * N17 - MLS
 * N18 - MLS
 * N19 - MLS

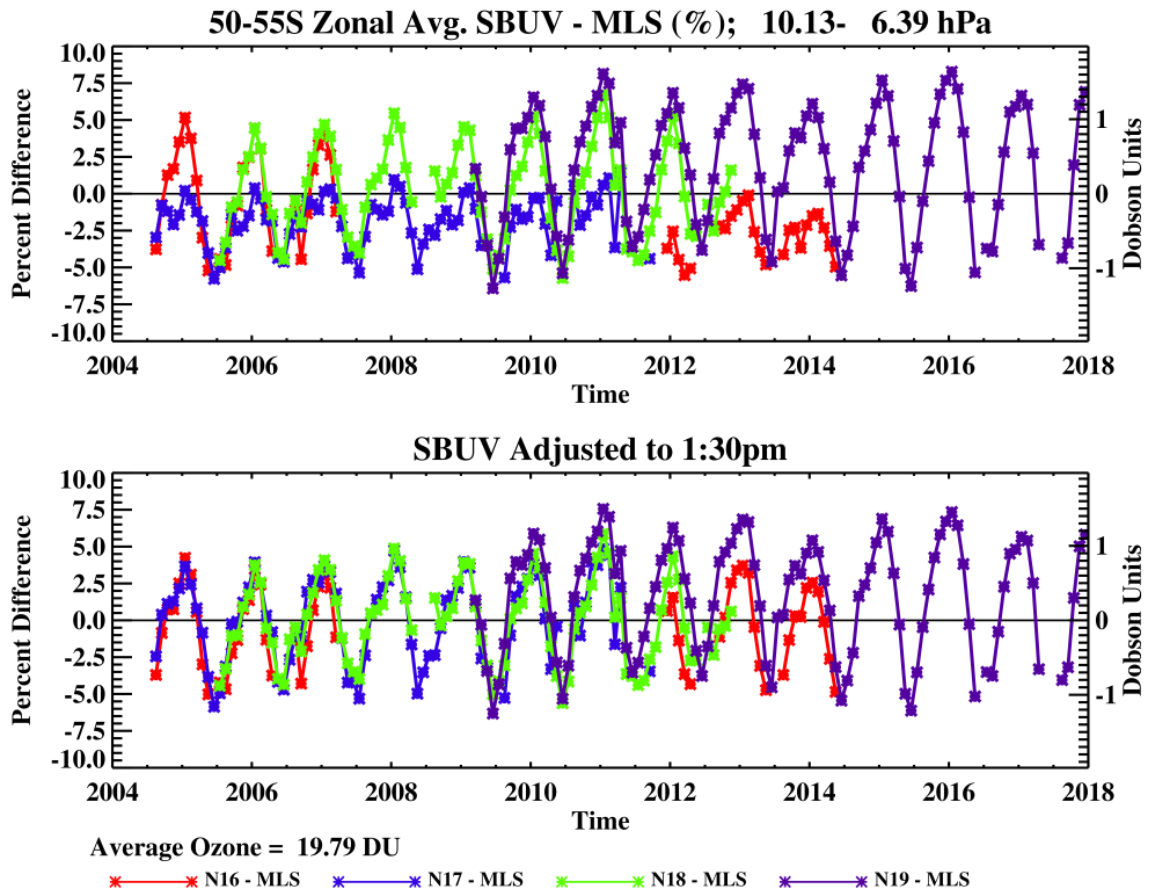


Figure 12. Figure 11. Same as Figure 1011 but for 50-55° S latitude band at 10-6.4 hPa layer.